ASSESSMENT REPORT TITLE PAGE AND SUMMARY

TITLE OF REPORT: Report on a Helicopter-Borne AeroTEM System Electromagnetic, Magnetic Survey – Berg Project, Smithers, BC, Canada

TOTAL COST: $ 99,894.00

AUTHOR(S): **Darin Labrenz, P.Geo**
SIGNATURE(S):

NOTICE OF WORK PERMIT NUMBER(S)/DATE(S): N/A
STATEMENT OF WORK EVENT NUMBER(S)/DATE(S): **4810197**

YEAR OF WORK: **2010**

PROPERTY NAME: **Berg**

CLAIM NAME(S) (on which work was done): **515449,515450,515451,594483,594490,594495, 515338,515454,515455,515456,515447,671443,671444,671450,671451,671463,671467,671472, 671473,671484,671503,671523,671526,671527,673446,673465,673485,673503,673523,693844**

COMMODITIES SOUGHT: **Cu, Mo**

MINERAL INVENTORY MINFILE NUMBER(S),IF KNOWN: **093E-008, 046, 052**

MINING DIVISION: **Omineca**
NTS / BCGS: **093E/14**
LATITUDE: **53° 49' 00"**
LONGITUDE: **-127° 24' 00"** (at centre of work)
UTM Zone: **9N** EASTING: **609,000E** NORTHING: **5,964,000N**

OWNER(S): **Berg Metals Limited Partnership**

MAILING ADDRESS: **Suite 1500, 999 West Hastings Street, Vancouver, BC, V6C 2W2**

OPERATOR(S) [who paid for the work]: **Terrane Metals Corp.**

MAILING ADDRESS: **Suite 1500, 999 West Hastings Street, Vancouver, BC, V6C 2W2**

REPORT KEYWORDS (lithology, age, stratigraphy, structure, alteration, mineralization, size and attitude. **Do not use abbreviations or codes**)

Berg, Bergette, calc-alkalic porphyry, copper, molybdenum, 50 Ma quartz monzonite stock and quartz diorite intrusive, Jurassic Hazelton Group volcanic rocks

REFERENCES TO PREVIOUS ASSESSMENT WORK AND ASSESSMENT REPORT NUMBERS:
5429, 5500, 19749, 29578

TYPE OF WORK IN THIS REPORT	EXTENT OF WORK (in metric units)	ON WHICH CLAIMS	PROJECT COSTS APPORTIONED (incl. support)
GEOLOGICAL (scale, area)			
Ground, mapping			
Photo interpretation			
GEOPHYSICAL (line-kilometres)			
Ground			
Magnetic			
Electromagnetic			
Induced Polarization			
Radiometric			
Seismic			
Other			
Airborne	**754 line-km**	see page 1	**$ 99,894**
GEOCHEMICAL (number of samples analysed for …)			
Soil			
Silt			
Rock			
Other			
DRILLING (total metres, number of holes, size, storage location)			
Core			
Non-core			
RELATED TECHNICAL			
Sampling / Assaying			
Petrographic			
Mineralographic			
Metallurgic			
PROSPECTING (scale/area)			
PREPATORY / PHYSICAL			
Line/grid (km)			
Topo/Photogrammetric (scale, area)			
Legal Surveys (scale, area)			
Road, local access (km)/trail			
Trench (number/metres)			
Underground development (metres)			
Other			
		TOTAL COST	**$ 99,894**

Terrane METALS CORP. | a Subsidiary of Thompson Creek Metals Company

Report on a Helicopter-Borne AeroTEM System Electromagnetic-Magnetic Survey on the Berg Property

Tahtsa Range, central British Columbia
Omineca Mining Division
NTS Mapsheet 93E/14

Centred at:
53°49' N Latitude / 127°24' W Longitude

Owner:

Berg Metals Limited Partnership
Suite 1500 – 999 West Hastings Street
Vancouver, B.C. Canada
V6C 2W2

Operator:

Terrane Metals Corp
Suite 1500 – 999 West Hastings Street
Vancouver, B.C. Canada
V6C 2W2

Prepared by:

Darin Labrenz, B.Sc., P. Geo.
Director Exploration – **Terrane Metals Corp**

January 2011

Table of Contents

List of Tables

List of Figures

List of Appendices

Introduction

Aeroquest International conducted a helicopter-borne geophysical survey on behalf of Terrane Metals Corp., over the Berg property between August 8th and August 14th, 2010. This survey utilized Aeroquest's AeroTEM III time domain helicopter electromagnetic system in conjunction with a high-sensitivity caesium vapour magnetometer. The total survey coverage is 754.35 line-km, flown at 100 metre line spacing and in 90°/270° flight direction.

The objective of the survey was to map the magnetic and conductive properties of the Berg property, with the aim of increasing geologic knowledge, and identifying anomalies similar to those expressed by the Berg Deposit.

Location and Access

The Berg Property is located in the Omineca Mining Division within the Tahtsa Ranges of West Central British Columbia, approximately 84 km southwest of Houston and 22 km northwest of Imperial Metals Corporation's Huckleberry Mine (Figure 1). The property is comprised of 54 mineral claims and one mining lease centered at 53° 49' North Latitude and 127° 24' West Longitude. The Berg deposit area is located near UTM Zone 9, NAD 83, 603330 m East and 5962700 m North.

Access to the Berg Property during historic exploration prior to 1980 was by way of a 42 km four-wheel drive road from Twinkle Lake on the Tahtsa Lake Forest Service Road. The old access road crosses the north flank of Sibola Peak and follows Kidprice Creek south and west to a 1,740-metre high pass at its headwaters. The Berg deposit is located on a tributary to the north fork of Bergeland Creek, about 6 km northwest of the pass at an elevation of 1,555 m. Depending upon yearly snow accumulations, the route is generally free of snow between July and October. A portion of the four-wheel drive road was upgraded for logging and is accessible for loaded trucks to a laydown and borrow pit 20 kilometres east-northeast of the Berg deposit.

Figure 1 Berg Location Map

Property Description and Ownership

The Berg property is 100% owned by Berg Metals Limited Partnership with a 1% Net Smelter Return Royalty to International Royalty Corporation, a wholly owned subsidiary of Royal Gold Inc. The Berg property consists of 54 mineral claims and one mining lease for a total of 19,655 hectares (Figure 2). The mineral claims are in good standing until November 10, 2011 and no further filing or payments are required on them until that date.

The single mining lease was issued on August 27, 1968 and has required lease payments of $169.10 due annually by August 27. The legacy mining lease expires in 2019 and has been completely overstaked by the mineral claims. Mining leases in BC are title granting mineral production based on the surveyed area. The lease covers the NE corner of the Berg deposit (Figure 2).

Table 1 Berg Claim Status

Tenure Number	*Claim Name*	*Owner*	*Tenure Type*	*SubType*	*Map Number*	*Expiry Date*	*Area (ha)*
243481*		248461 (100%)	Mineral	Lease	093E083	2011/aug/27	16.81
515447*		248461 (100%)	Mineral	Claim	093E	2017/oct/15	191.004
515449*		248461 (100%)	Mineral	Claim	093E	2017/oct/15	190.966
515450*		248461 (100%)	Mineral	Claim	093E	2017/oct/15	572.74
515451*		248461 (100%)	Mineral	Claim	093E	2017/oct/15	553.588
515453*		248461 (100%)	Mineral	Claim	093E	2017/oct/15	477.444
515454*		248461 (100%)	Mineral	Claim	093E	2017/oct/15	496.524
515455*		248461 (100%)	Mineral	Claim	093E	2017/oct/15	229.252
515456*		248461 (100%)	Mineral	Claim	093E	2017/oct/15	343.875
545074	SOUTH 1	248461 (100%)	Mineral	Claim	093E	2011/nov/10	287.0966
545075	SOUTH 2	248461 (100%)	Mineral	Claim	093E	2011/nov/10	363.5405
545076	SOUTH 3	248461 (100%)	Mineral	Claim	093E	2011/nov/10	401.6407
545077	SOUTH 4	248461 (100%)	Mineral	Claim	093E	2011/nov/10	401.6379
545078	SOUTH 5	248461 (100%)	Mineral	Claim	093E	2011/nov/10	401.6389
545079	SOUTH 6	248461 (100%)	Mineral	Claim	093E	2011/nov/10	401.7575
545080	SOUTH 7	248461 (100%)	Mineral	Claim	093E	2011/nov/10	344.3572
545081	SOUTH 8	248461 (100%)	Mineral	Claim	093E	2011/nov/10	459.149
545082	SOUTH 9	248461 (100%)	Mineral	Claim	093E	2011/nov/10	459.2846
545083	SOUTH 10	248461 (100%)	Mineral	Claim	093E	2011/nov/10	325.4207
545084	SOUTH 11	248461 (100%)	Mineral	Claim	093E	2011/nov/10	363.7019
545085	SOUTH 12	248461 (100%)	Mineral	Claim	093E	2011/nov/10	229.6488
545086	SOUTH 13	248461 (100%)	Mineral	Claim	093E	2011/nov/10	306.1689
545087	SOUTH 14	248461 (100%)	Mineral	Claim	093E	2011/nov/10	401.8809
594483	BERG C	248461 (100%)	Mineral	Claim	093E	2012/nov/30	477.7854
594485	BERG D	248461 (100%)	Mineral	Claim	093E	2012/nov/30	477.9961
594490	BERG A	248461 (100%)	Mineral	Claim	093E	2012/nov/30	477.839
594495	BERG I	248461 (100%)	Mineral	Claim	093E	2012/nov/30	458.028
604970		248461 (100%)	Mineral	Claim	093E	2012/nov/30	478.1444
604976		248461 (100%)	Mineral	Claim	093E	2012/nov/30	191.3234
604978		248461 (100%)	Mineral	Claim	093E	2012/nov/30	478.2371
671443		248461 (100%)	Mineral	Claim	093E	2012/nov/30	477.3702
671444		248461 (100%)	Mineral	Claim	093E	2012/nov/30	458.1384
671450		248461 (100%)	Mineral	Claim	093E	2012/nov/30	477.0649
671451		248461 (100%)	Mineral	Claim	093E	2012/nov/30	477.0645
671463		248461 (100%)	Mineral	Claim	093E	2012/nov/30	381.64
671467		248461 (100%)	Mineral	Claim	093E	2012/nov/30	228.9265
671472		248461 (100%)	Mineral	Claim	093E	2012/nov/30	114.5628
671473		248461 (100%)	Mineral	Claim	093E	2012/nov/30	229.1254
671484		248461 (100%)	Mineral	Claim	093E	2012/nov/30	248.3239
671503		248461 (100%)	Mineral	Claim	093E	2012/nov/30	477.5783
671523		248461 (100%)	Mineral	Claim	093E	2012/nov/30	95.5252
671526		248461 (100%)	Mineral	Claim	093E	2012/nov/30	191.0128

Tenure Number	Claim Name	Owner	Tenure Type	SubType	Map Number	Expiry Date	Area (ha)
671527		248461 (100%)	Mineral	Claim	093E	2012/nov/30	381.8585
672023		248461 (100%)	Mineral	Claim	093E	2012/nov/30	305.6054
673446		248461 (100%)	Mineral	Claim	093E	2012/nov/30	381.6526
673465		248461 (100%)	Mineral	Claim	093E	2012/nov/30	190.9192
673485		248461 (100%)	Mineral	Claim	093E	2012/nov/30	95.4597
673503		248461 (100%)	Mineral	Claim	093E	2012/nov/30	343.8404
673523		248461 (100%)	Mineral	Claim	093E	2012/nov/30	95.4132
693843		248461 (100%)	Mineral	Claim	093E	2012/nov/30	457.5074
693844		248461 (100%)	Mineral	Claim	093E	2012/nov/30	476.8043
693883		248461 (100%)	Mineral	Claim	093E	2012/nov/30	457.5136
693884		248461 (100%)	Mineral	Claim	093E	2012/nov/30	457.5066
693903		248461 (100%)	Mineral	Claim	093E	2012/nov/30	457.5093
693904		248461 (100%)	Mineral	Claim	093E	2012/nov/30	438.6436

(*) Tenures with 1% NSR Royalty

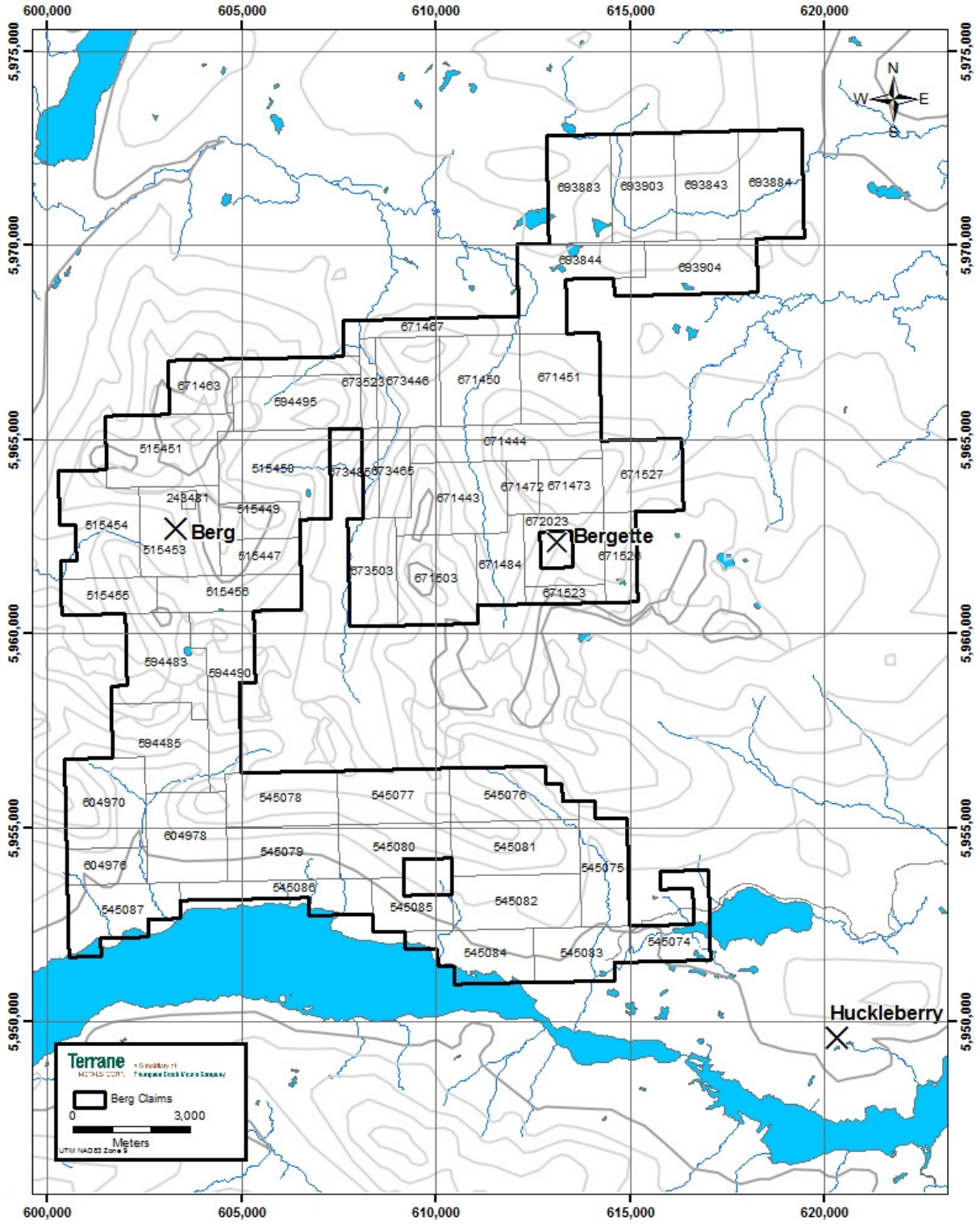

Figure 2: Berg Property - Tenure Map

Property History

The Tahtsa Ranges were first prospected in the early 1900's after gold was discovered near Sibola Mountain. Prior to the late 1920's, several lead-zinc-silver, gold-tungsten and copper showings had been staked. In 1948, the Lead Empire Syndicate re-staked claims originally located in 1929 by Cominco Ltd. over several lead-zinc occurrences. These are now recognized as part of the Berg porphyry system.

The potential for porphyry copper style mineralization at Berg was first understood by Kennco (Kennecott), based on their experience in the southwestern United States. Increased exploration expenditures in 1964 enabled bulldozer trenching and diamond drilling that demonstrated the deep effects of surface leaching and revealed the widespread presence of supergene mineralization, a feature not common in the Canadian Cordillera. Subsequent work shows that rocks are leached in places to depths in excess of 30 metres, and these rocks are underlain by an extensive "blanket" of supergene copper enrichment.

Drilling by Kennecott during 1965 and 1966 delineated two main mineralized zones. A northeast zone contains primary (hypogene) and some supergene mineralization, and a southeast zone has widespread supergene and lesser hypogene mineralization. At the end of the 1966 field season, the property consisted of 108 mineral claims on which there had been a total of 3886 metres of diamond drilling in 23 holes. During 1967, a 3325 metre drill program tested the southeast zone on a widely-spaced grid and three holes explored areas peripheral to the Berg deposit. From 1968 to 1970 the property was dormant but metallurgical testing was completed on composite samples of drill core. In 1971, three additional holes were drilled in the northeast zone. At the end of the 1971 exploration program a total of 49 diamond-drill holes of mainly NQ and BQ core had been completed with a total length of 7875.8 meters.

In 1972, exploration and development of the property were taken over by Canex Placer Limited (Placer Dome Inc.) under agreement with Kennecott. From 1972 to 1975, Placer Dome drilled an additional 52 core holes of NQ and PQ core totalling 9689.4 metres. The PQ holes were utilized to collect metallurgical samples and to address low core recovery issues from previous years. Another 8 HQ core holes totalling 1099.0 metres were drilled in 1980.

A total of 119 diamond drill holes for 20,127.9 metres were completed by 1980 on the Berg property. Of these, 93 drill holes for 16,907.8 metres are in the deposit area and were used in historical resource estimates. A limited amount of the old drill core is still cross-stacked on the property, but most of the mineralized sections have been consumed for metallurgical test-work and core box identification is sometimes difficult due to their deteriorating condition over the years.

Between 1982 and 2007, there was no active exploration on the project, although Placer had arranged for or conducted in-house revised resource estimates, additional economic analyses, conceptual mine layouts, and environmental reports. No mining activity has occurred on the property.

In 2006, Placer Dome was purchased by Barrick Gold, who sold the Canadian assets to Goldcorp Inc. Terrane Metals Corp (Terrane) purchased certain Canadian assets from Goldcorp, including

their share of the Berg project. In September 2006, Terrane purchased Kennecott's share of the Berg joint venture to become 100% owners.

In 2007 Terrane reactivated exploration on the Berg Property with a 29 drill hole program totalling 11,289 metres. The program was designed to confirm historical drill hole results. The information was utilized in the first NI 43-101 compliant resource estimate which was published April 2008.

In 2008, Terrane completed an addition 31 diamond drill holes totalling 11,661 m to refine the deposit's geological model, upgrade resources from the Inferred to Measured and Indicated categories, confirm historic assay results, and test prospective areas outside the limits of previous drilling. A revised NI 43-101 resource estimate was published May 2009. To date a total of 43,076.4 metres have been drilled in 179 holes.

Geology

Regional Geology

The Berg deposit, located in the western portion of the Berg property, is centered on one of several Early to Middle Eocene (52 Ma to 47 Ma) composite quartz monzonite stocks that intrude Middle Jurassic Hazelton Group and Lower Cretaceous Skeena Group rocks in the area. Hazelton Group rocks are well exposed west of the Berg stock. They consist of a sequence of green, grey, red and maroon lithic tuffs, tuff breccias and flows of andesitic composition. Skeena Group rocks overlie the Hazelton Group and are exposed mainly east of the deposit. Amygdaloidal and vesicular andesites and basalts make up the lower part of the Skeena Group succession. Many of the flows exhibit trachytic texture that distinguishes them from the underlying Hazelton Group. Sandstones, siltstones and conglomerates comprise the upper part of the succession.

The contact between the Skeena Group and the Hazelton Group is not exposed in the property area as it is everywhere intruded by quartz diorite. An exposure of the contact on a cliff face north of the Berg property is strongly epidotized and rocks on both sides are hydrothermally altered. Kasalka Group rocks uncomformably overlie the Skeena Group north of the property. Best exposures occur at Mount Ney, 6 km north of the Berg stock. Here the succession consists of a basal conglomerate member that has a distinctive red to maroon colour. Overlying the conglomerate is a predominantly volcanic sequence of white, grey and pale green rhyolite and dacite flows and flow breccias with interbedded crystal and crystal vitric tuff.

Structure in the area consists of poorly developed open folds with north to northeast axial trends causing local dips of 10^{o} to 30^{o}. Fractures and Miocene basalt dikes parallel this structural trend that may have acted as the principal structural control for the emplacement of intrusions in the area. This relationship is supported by the pronounced elongation of the quartz diorite intrusion.

Refer to Figure 3 for the BCGS Regional Geology map showing bedrock geology and the Berg Property.

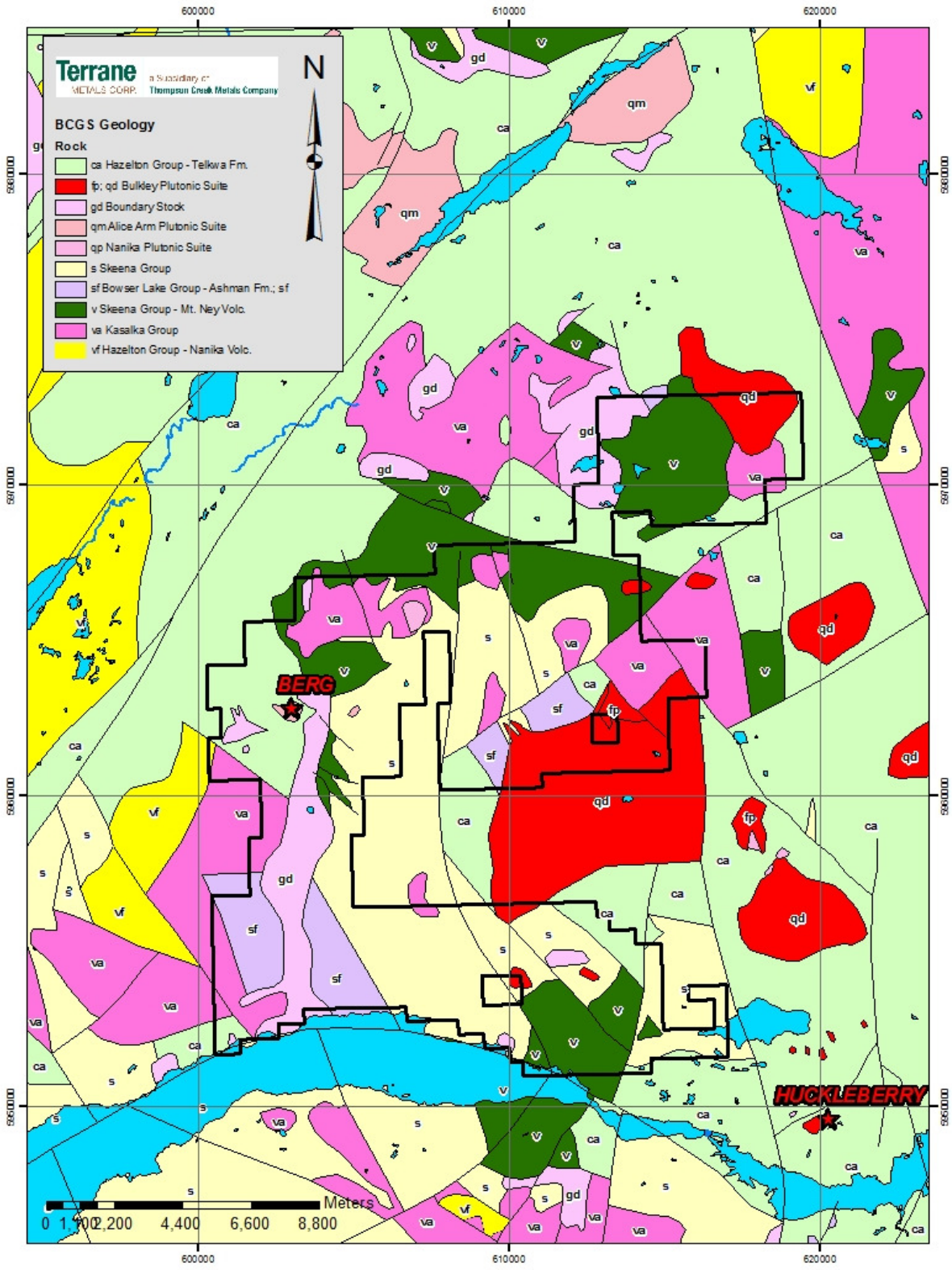

Figure 3 Regional Geological Setting of the Berg Property

Local Geology

The Berg Deposit has been well studied with excellent treatises on the geology, alteration and mineralization by Panteleyev (1976, 1981), Heberlein and Godwin (1984), and Heberlein (1995); the following description is largely based upon their work. Two main intrusive bodies are exposed in the property area. The largest consists of a north-trending, elongate body of quartz diorite (**Unit QDR**) that intrudes the contact between Hazelton Group and Skeena Group east of the mineralized area. The intrusion extends from about 750 metres north of the Berg Stock to over 6.5 km to the south (see Figures 3 and 4). It ranges in width from 600 metres on the property area to over 2 km at its southern extremity. Compositional and textural zonation of the quartz diorite is evident with a central core of pink quartz monzonite exposed 1.6 km south of the camp that grades outwards into quartz diorite and hornblende quartz diorite. Porphyritic phases are also present. At hand-specimen scale the quartz diorite is fine-grained and pale grey or dark grey-brown where hornfelsed or biotite-altered. This unit is a fine-grained equigranular rock consisting of plagioclase, hornblende, biotite and quartz overprinted by biotite, chlorite and minor epidote alteration. Where the quartz diorite is mineralized, quartz veining, chalcopyrite, pyrite and molybdenite are present in association with biotite alteration. This grades outwards into biotite-chlorite±epidote alteration with pyrite overprinting primary magnetite. A well developed thermal aureole up to 120 m wide occurs on both sides of the intrusion and into Hazelton Group andesitic rocks in the deposit area. The western contact of the quartz diorite and Hazelton Group andesitic rocks is subvertical and diffuse in nature in the deposit area due to the nature of the hornfelsing and overprinting alteration. Hornfelsed rocks are typically brownish purple due to the abundance of secondary biotite.

The other prominent intrusion in the deposit area is the Berg Stock, a multi-phase composite quartz monzonite stock that intrudes the Hazelton Group andesitic rocks. It is broadly cylindrical and approximately 600 to 750 m in diameter with typically sharp, subvertical contacts. Locally these contacts are complex with brecciated xenoliths of andesitic rocks with diffuse clast boundaries. This stock is the prime control on mineralization at the Berg as the deposit forms an annulus around the stock. Panteleyev (1976, 1981) subdivided this composite stock into four main phases:

a) a core of pre-mineral, very coarsely porphyritic quartz monzonite (**Unit QMP**),
b) a pre-mineral coarse-grained plagioclase-biotite-quartz porphyry (**Unit PBQP**) that wraps around the northern flank of the QMP core,
c) a northwest-trending, pre-mineral medium-grained weakly porphyritic quartz-plagioclase porphyry (**Unit QPP**) that extends to the west from the southern and western portion of the QMP core,
d) narrow, subvertical, northwest- and northeast-trending late- to post-mineral quartz-feldspar porphyry (**Unit QFP**) dykes or zones of dyking that cut across each of the above phases and also cut quartz diorite along trend and northeast of the stock and,
e) late- to post-mineral potassium feldspar megacrystic quartz monzonite porphyry dykes (**Unit KQMP**).

Unit QMP is characterized by very coarse-grained plagioclase, quartz, biotite and commonly megacrystic orthoclase. The quartz in particular is distinctive, commonly comprising coarse resorbed crystals with subrounded and wormy boundaries and with poikilitic intergrowths of plagioclase. Feldspars and biotites are euhedral and minor hornblende is typically replaced by biotite.

The **PBQP** is a slightly finer-grained quartz monzonite than the QMP with a typically darker grey to brown matrix containing plagioclase, quartz and biotite with rare orthoclase. Biotite is roughly twice as abundant and typically finer-grained than in the QMP, comprising 2 mm books compared with the 4-6 mm books in unit QMP. Internal contacts and cross-cutting relationships within the Berg Stock between the PBQP and the QMP are poorly understood due to lack of drilling, but contacts with the andesitic country rocks appear to be largely sub-vertical.

Unit QPP is also quartz monzonitic in composition and has the finest grain size of the Berg Stock phases. This leucocratic phase is medium-grained, comprising mainly plagioclase and quartz with notably absent or rare orthoclase and biotite. The QPP also exhibits characteristically strong and pervasive sericite alteration and local fine secondary biotite. This unit appears to cut the QMP and appears to have a strong degree of structural control in its emplacement forming a west-northwest trending subvertical keel along the southern margin of the stock.

The **QFP** dyke forms the backbone of the northeast-trending ridge that transects the Berg Deposit. This dyke is also very coarse-grained, closely resembling the QMP with coarse-grained plagioclase, biotite, resorbed and subrounded quartz, hornblende and minor orthoclase megacrysts. Distinctive coarse-grained crystals of sphene are also present. Plagioclase is altered to sericite, carbonate and trace epidote and orthoclase megacrysts are also altered by epidote. Mafic phases are altered to chlorite, calcite, epidote, rutile and hematite. Quartz-pyrite±chalcopyrite veining (Stage 3) is locally present and quartz-molybdenite (Stage 1) and quartz-pyrite-chalcopyrite-molybdenite veining (Stage 2) are rare within the QFP. Veining in the QFP typically occurs within mineralized xenoliths of andesite, quartz diorite or earlier phases of the stock. This unit is also the only phase of the Berg Stock that intersects the quartz diorite. This dyke narrows or bifurcates to only a few metres wide where it has been intersected by drilling at the southwest and northeast margins of the stock.

Unit **KQMP** is another late mineral intrusive phase that has been noted in drill core only. It is also strongly similar to the QMP with coarse-grained plagioclase, resorbed and myrmekitic quartz, biotite and more abundant (>2%) megacrystic orthoclase. This unit is typically weakly altered with weak sericite±carbonate alteration of plagioclase and biotite, and local K-feldspar and biotite alteration of these primary phases. Like the QFP, mineralized quartz veining is scarce and commonly occurs in mineralized xenoliths. Contacts of the KQMP and QFP with other phases of the stock, quartz diorite and andesite are typically sharp, although contacts between the KQMP and QFP have been observed to be gradational. At depth in the central portion of the Berg stock, the QFP appears to grade into KQMP. A KQMP dyke has also been observed trending southeasterly across the southwestern portion of the Berg stock, sub-parallel to part of the QPP.

Dark green, typically fine-grained to aphanitic andesite dykes (**Unit ANDD**) cut all units. These dykes are typically very narrow and comprise plagioclase and hornblende with accessory magnetite and calcite amygdales. Where observed in outcrop they are steeply southwest-dipping and southeast-striking, although a northeasterly orientation, parallel to the main QFP dyke zone is also probable. They are particularly common in the Northeast Zone and appear to be coincident with narrow zones of faulting and clay±sericite alteration, particularly along dyke contacts.

These various intrusive phases intrude Hazelton Group volcanic and sedimentary rocks; comprising subaerial to subaqueous medium- to coarse-grained andesitic lapilli tuffs (**Units ANTF** and **ANLT**) and lesser flows (**Unit ANDF**), breccias and volcaniclastic sediments (**Unit GRWK**). Minor shale (**Unit SHAL**), siltstone (**Unit SLST**), chert (**Unit CHRT**) and limestone (**Unit LMST**) are also present. Outside the area of influence of the quartz diorite and the Berg Stock these Hazelton Group rocks vary from dark grey to grey-green, purple and red with obvious textures and bedding. Within the alteration aureoles of the intrusions, primary textures are largely obscured or rocks are recrystallized and dark grey or brown in colour. Relict clasts and phenocrysts are locally recognized within the alteration haloes. This succession strikes roughly north and dips shallowly to moderately to the east and is tops-up.

Alteration and mineralization at Berg is localized in and adjacent to the quartz monzonite Berg Stock. Mineralization occurs in a highly fractured zone superimposed on hornfelsed Hazelton Group andesitic volcanic rocks, the adjacent quartz diorite intrusion and, to a lesser degree, the Berg Stock (Figure 4).

Hydrothermal alteration zones are spatially related to the central quartz monzonite stock and extend up to 1000 m from the intrusive contact. Alteration types are divided into potassic, phyllic, argillic and propylitic facies whose diagnostic mineral assemblages vary with lithology.

Potassic alteration is expressed as pervasive orthoclase alteration in unit QMP, orthoclase on fracture/veinlet selvages and pervasive fine-grained biotite in the matrix of the PBQP, and pervasive fine-grained biotite alteration and replacement of mafic minerals in the quartz diorite and andesite. A subzone of biotite alteration with anhydrite veining lies proximal to the inner contact of this biotite-altered zone against the Berg Stock. This phase of alteration is also associated with the replacement of plagioclase phenocrysts in the Berg Stock. On a mesoscopic scale orthoclase is also observed in the selvages of Stage 1 veins.

Similar to the zone of biotite alteration, propylitic alteration is also concentrically zoned about the Berg Stock; a transitional zone of biotite-chlorite alteration lies inboard of a zone of chlorite-epidote-carbonate-albite as biotite decreases. Primary magnetite is also present, particularly within the biotite-chlorite zone, where not completely sulphidized to pyrite and chalcopyrite. Fracture-controlled retrograde chlorite-epidote-carbonate alteration is also present overprinting other alteration facies as the hydrothermal system collapsed. Chlorite, epidote, calcite and hematite present in the late-mineral QFP dykes and carbonate-chlorite-sphalerite-pyrite veins are likely also related to this retrograde event.

Two phyllically-altered zones have been observed in the Berg project area. An inner phyllic zone is best developed in all units around the margins of the Berg Stock and is dominantly controlled by fractures with quartz and pyrite and sericite-altered selvages. Where fracture densities are greatest this fracture selvage-controlled alteration can be pervasive as in the QPP and in portions of the QMP. A second phyllic zone comprising fracture-controlled quartz, sericite and pyrite has been identified within quartz diorite and andesite in the easternmost holes in the Northeast and South Zones. This phyllic zone is located peripherally to the biotite-chlorite zone and inward of the more widespread chlorite-epidote alteration and sharply truncates Cu mineralization.

A cap of pervasive kaolinite-clay±silica (argillic alteration) overprints potassic and phyllic alteration within the supergene zone and is likely related to acidic solutions formed from the breakdown of pyrite.

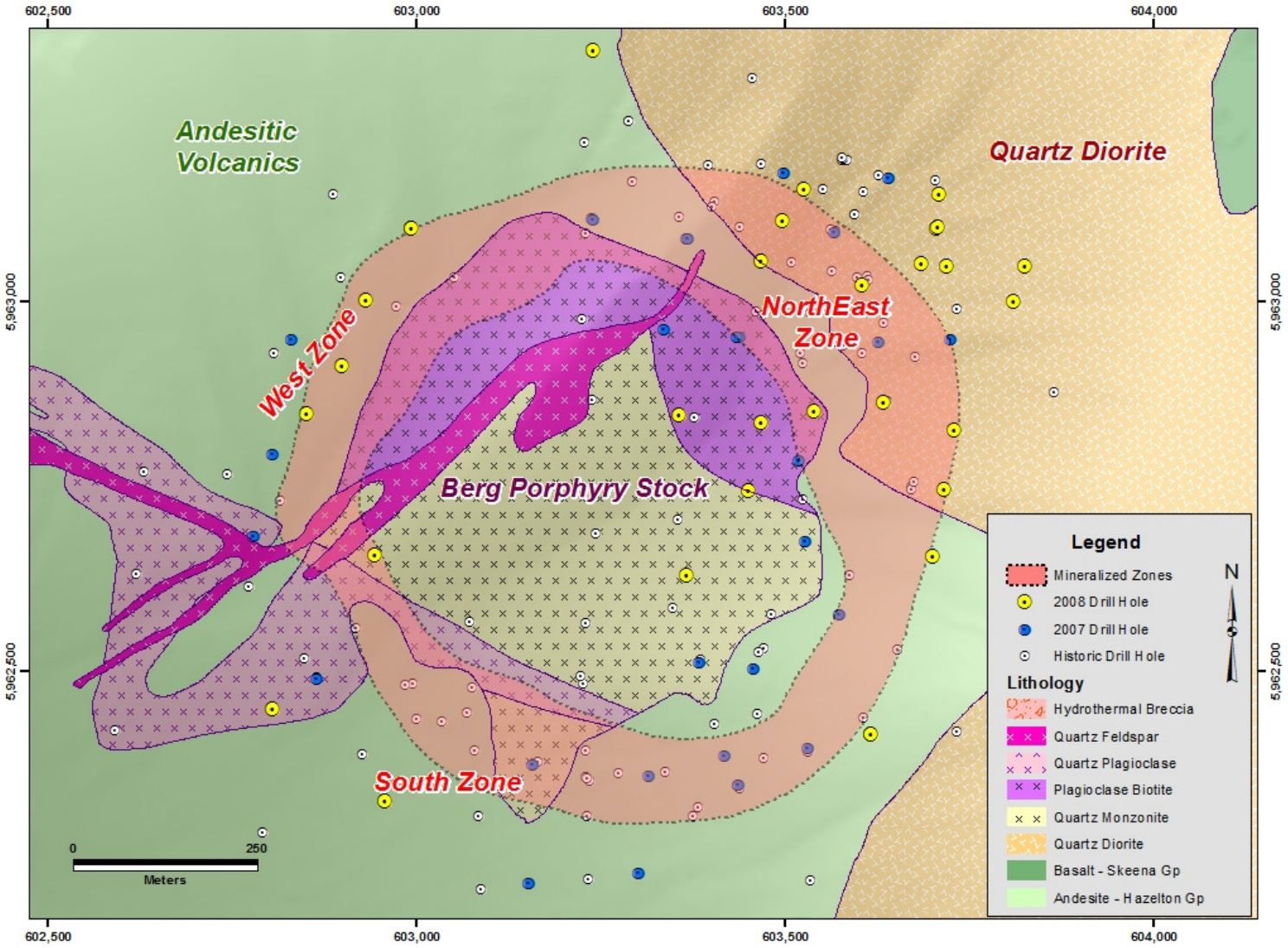

Figure 4 Local Geology of the Berg Deposit

2010 Work Program

Aeroquest International conducted a helicopter-borne geophysical survey on behalf of Terrane Metals Corp., over the Berg property between August 8th and August 14th, 2010. This survey utilized Aeroquest's AeroTEM III time domain helicopter electromagnetic system in conjunction with a high-sensitivity caesium vapour magnetometer. The total survey coverage is 754.35 line-km, flown at 100 metre line spacing and in 90°/270° flight direction.

Navigation was carried out using a GPS receiver, an AGNAV2 system for navigational control, and AeroDAS data acquisition system which records the GPS coordinates. On return to base, AeroDAS streaming EM and ancillary data were removed and transferred to computer where data verification and quality control measures were completed. In the event of excessive deviation from intended flight-path, or where quality control issues were identified, survey lines were re-flown.

The AeroTEM III survey employed a Geometrics G-823A caesium vapour magnetometer sensor contained within a two metre towed bird airfoil attached to the main tow line, 38.1 metres above the EM bird. The nominal ground clearance of the magnetometer is 68.1 metres, and magnetic data is recorded at 10 Hz by the ADAS.

The electromagnetic system is an Aeroquest AeroTEM III time domain towed-bird system, which is towed 56.1 metres below the helicopter. More technical details on the magnetometer and EM systems can be found in Appendix 1.

Discussion of Results

The survey was successful in mapping the magnetic and conductive properties of the Berg property.

The magnetic survey maps out the magnetic properties of the underlying geology, and can be used to map out geologic structures, and contacts. The QDR unit, located immediately west of the Berg deposit, exhibits a strong magnetic response, whereas the Berg deposit exhibits a more subtle response. Similar features can be mapped in other areas of the map sheet.

The EM anomalies are related to conductance, as well as thickness of the source. The Berg deposit is mapped by a distinctive EM halo. Similar anomalies can be located within the surveyed area.

Conclusions

The AeroTEM III survey was successful in mapping the magnetic and conductive properties of the Berg property. This survey has provided a geophysical signature for the underlying geology, and for the known Berg deposit. Further work is required to incorporate the geophysical data into geological interpretations of the surveyed area. This information will further understanding of the Berg deposit, and will be used to target similar alteration patterns across the property.

References

Awmack, H. (2006); Berg Site Visit; Memorandum to Terrane Metals Corp.; September 11, 2006 (unpublished)

Awmack, H. and O'Brien, D. (2007); Technical Report on the Berg Copper-Molybdenum-Silver Property

Boyce, R.A. (1983); Berg Regional Geology and Geochemistry Program (unpublished)

Cannon, R. W., and Pentland, W.S. (1981); 1980 Exploration Report – Sun Mineral Claims.

Drummond, A.D. et al. (1975); Berg Property – Progress Report (unpublished)

Dumas, K. and O'Brien, D. (2008); 2007 Aerial Photogrammetric Report on the South Berg Property; assessment report for the British Columbia Ministry of Energy, Mines and Petroleum Resources

Harris, S. (2008); 2007 Diamond Drilling Report on the Berg Property; assessment report for the British Columbia Ministry of Energy, Mines and Petroleum Resources

Harris, S. and Stubens, T. (2008); Technical Report – Mineral Resource Estimate, Berg Property, Tahtsa Range, British Columbia; NI43-101 Technical Report prepared for Terrane Metals Corp; June 2008

Harris, S. and Labrenz, D. (2009); Technical Report – 2009 Mineral Resource Estimate on the Berg Copper-Molybdenum-Silver Property, Tahtsa Range, British Columbia; NI43-101 Technical Report prepared for Terrane Metals Corp; June 2009

Heberlein, D.R. (1985); Hydrothermal alteration and rock geochemistry at the Berg porphyry copper-molybdenum deposit, north-central British Columbia, Unpublished M.Sc. Thesis, UBC, 99 pp.

Heberlein, D.R. (1995); Geology and supergene processes: Berg copper-molybdenum porphyry, west-central British Columbia, Porphyry Deposits of the Northwestern Cordillera of North America CIM Special Volume 46, pp 304-312.

Heberlein, D.R. and Godwin, C.I. (1984); Hypogene alteration at the Berg property

Huston, D. R. and Beaudoin, P.G. (1974); Report on Exploration Activity at the Berg Project

MacIntyre, D.G., Ash, C. and Britton, J., (1994): Nass-Skeena (93/E, L, M; 94/D; 103/G, H, I, J, P; 104/A, B), Ministry of Energy, Mines and Petroleum Resources, Open File 1994-14

Mineral Services Canada Inc. (2008); Report No. MSC08/43R, Petrography of 8 Samples from the Berg Project (B.C.); Private Report prepared for Equity Engineering Ltd. and Terrane Metals Corp

Panteleyev, A. (1976); Geological setting, mineralization, and aspects of zoning at the Berg property copper-molybdenum deposit, central British Columbia, Unpublished Ph.D. Thesis, UBC, 235 pp.

Panteleyev, A., Drummond, A.D. and Beaudoin, P.G. (1976); Berg in Porphyry Deposits of the Canadian Cordillera, CIM Special Volume 15, pp 274-283.

Panteleyev, A. (1981); Geological setting, mineralization, zoning, and pyrite geochemistry, Berg project

PetraScience Consultants Inc. (2006); Petrography Report, Berg Property, BC, Project TMC06-01; Prepared for Henry Awmack, P.Eng., Equity Engineering Ltd.; November 22, 2006.

I, Darin Labrenz, of Garibaldi Highlands, British Columbia, do hereby certify that as the author of this report called “Report on a Helicopter-Borne AeroTEM SystemElectromagnetic-Magnetic Surveyon the Berg Property” dated January, 2011, I hereby make the following statements:

- I am Director Exploration with Terrane Metals Corp. with a business address at 1500 – 999 West Hastings Street, Vancouver, British Columbia.
- I am a graduate of University of Alberta, (B.Sc. Geology, 1987) and University of Alberta (Specialization Certificate, Computing Science, 1993).
- I am a member in good standing of the Association of Professional Engineers and Geoscientists of the Province of British Columbia as Member – Reg. No. 31529
- I have practiced my profession for a total of 20 years.
- My relevant experience with respect to geology includes working on a variety of mining and exploration projects in Canada, United States, Guyana, Chile, Malaysia and Tanzania over a total of 20 years.
- I am employed by and am not independent of Terrane Metals Corp.

Signed and dated this 26th day of January, 2011 at Vancouver, British Columbia

Darin M. Labrenz, P.Geo.

APPENDIX 1

LOGISTICS REPORT

Report on a Helicopter-Borne AeroTEM System Electromagnetic Magnetic Survey

Aeroquest Job # 10044

Berg Project
Smithers, B.C., Canada

For

Terrane Metals Corporation
Suite 1500-999 West Hastings,
Vancouver, B.C., Canada
V6C 2W2

by

7687 Bath Road,
Mississauga, ON, L4T 3T1
Tel: (905) 672-9129
Fax: (905) 672-7083
www.aeroquest.ca

Report date: November 2010

Report on a Helicopter-Borne AeroTEM System Electromagnetic, Magnetic Survey

Aeroquest Job # 10044

Berg Project
Smithers, B.C., Canada

For

Terrane Metals Corporation
Suite 1500-999 West Hastings,
Vancouver, B.C., Canada
V6C 2W2

by

7687 Bath Road,
Mississauga, ON, L4T 3T1
Tel: (905) 672-9129
Fax: (905) 672-7083
www.aeroquest.ca

Report date: November 2010

TABLE OF CONTENTS

LIST OF FIGURES

LIST OF MAPS (1:20,000)

- TMI – Total Magnetic Intensity (TMI) colour grid with line contours and EM anomaly symbols.
- ZOFF1– AeroTEM ZOff1-time colour grid with line contours and EM anomaly symbols.
- EM – AeroTEM off-time profiles and EM anomaly symbols.

1. INTRODUCTION

This report describes a helicopter-borne geophysical survey carried out on behalf of Terrane Metals Corporation, Berg project, near Smithers, B.C.

The principal geophysical sensor is Aeroquest's exclusive AeroTEM III (November) time domain helicopter electromagnetic system which is employed in conjunction with a high-sensitivity caesium vapour magnetometer. Ancillary equipment includes a real-time differential GPS navigation system, radar altimeter, video recorder, and a base station magnetometer. Full-waveform streaming EM data is recorded at 36,000 samples per second. The streaming data comprise the transmitted waveform, and the X component and Z component of the resultant field at the receivers. The streaming EM data along with ancillary data recorded with AeroDAS acquisition system.

The total survey coverage is 754.35 line-km, of which 744.33 line-km fell within the defined project area (Appendix 1). The survey was made up of one block, Berg Block, flown at 100 metre line spacing and in 90º/270º flight direction (Table 1). The survey flying described in this report took place from August 8th to August 14th, 2010. This report describes the survey logistics, the data processing, presentation, and provides the specifications of the survey.

2. SURVEY AREA

The Project area (Figure 1) is located in B.C. approximately 100 kms south of Smithers, B.C. The survey consisted of one block, Berg (132.92 km²). The base of survey operations was at Huckleberry Mines, B.C.

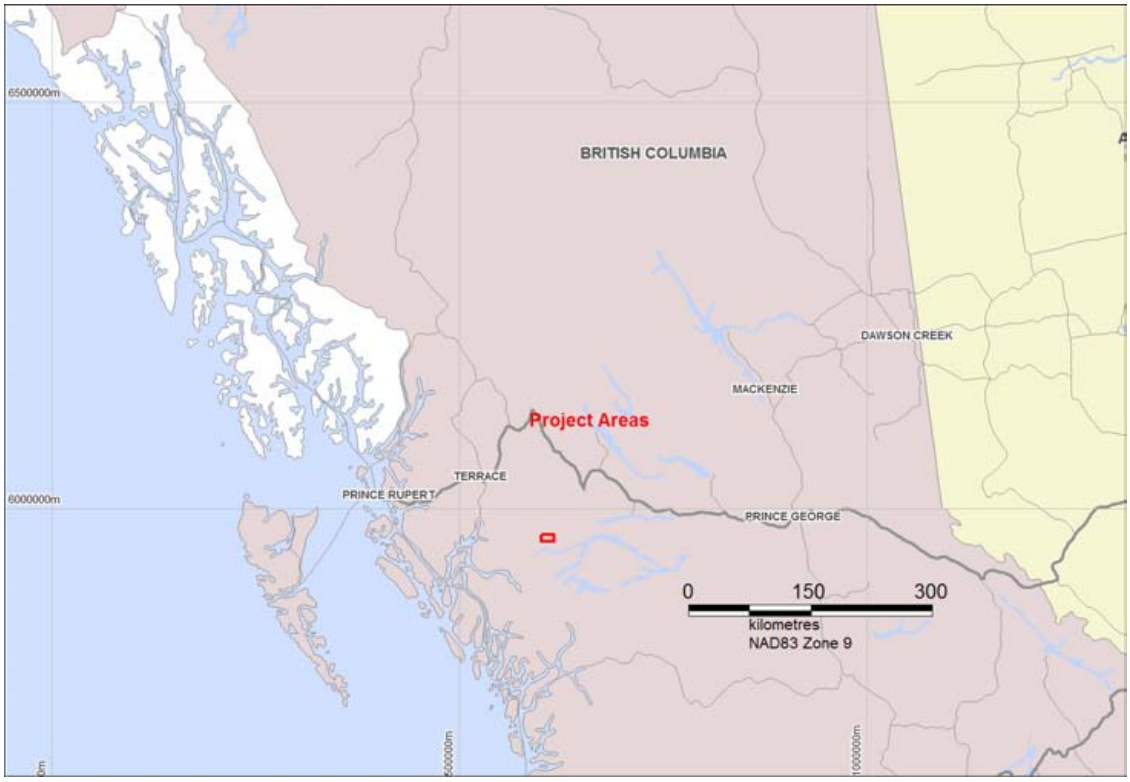

Figure 1. Project Area

3. SURVEY SPECIFICATIONS AND PROCEDURES

The survey specifications are summarised in the following table:

Project Name	Line Spacing (metres)	Line Direction	Survey Coverage (line-km)	Date flown
Berg	100	090º/270º	754km	Aug 8th to Aug 14th, 2010

Table 1. Survey specifications summary

The survey coverage was calculated by adding up the along-line distance of the survey lines and control (tie) lines as presented in the final Geosoft database. The survey was flown with a line spacing of 100 metres. The control (tie) lines were flown perpendicular to the survey lines with 2000 metre, tie line spacing.

The nominal EM bird terrain clearance is 30 metres, but can be higher in more rugged terrain due to safety considerations and the capabilities of the aircraft. The magnetometer sensor is mounted in a smaller bird connected to the tow rope 38.1 metres above the EM bird and 18 metres below the helicopter. Nominal survey speed over relatively flat terrain is 85 km/hr and is generally lower in rougher terrain. Scan rates for ancillary data acquisition is 0.1 second for the magnetometer and altimeter, and 0.2 second for the GPS determined position. The EM data is acquired as a data stream at a sampling rate of 36,000 samples per second and is processed to generate final data at 10 samples per second. The 10 samples per second translate to a geophysical reading about every 1.5 to 2.5 metres along the flight path.

3.1. NAVIGATION

Navigation is carried out using a GPS receiver, an AGNAV2 system for navigation control, and AeroDAS data acquisition system which records the GPS coordinates. The x-y-z position of the aircraft, as reported by the GPS, is recorded at 0.2 second intervals. The system has a published accuracy of less than 3 metres. A recent static ground test of the Mid-Tech WAAS GPS yielded a standard deviation in x and y of less than 0.6 metres and for z less than 1.5 metres over a two-hour period.

SYSTEM DRIFT

Unlike frequency domain electromagnetic systems, the AeroTEM III system has negligible drift due to thermal expansion. The operator is responsible for ensuring the instrument is properly warmed up prior to departure and that the instruments are operated properly throughout the flight. The operator maintains a detailed flight log during the survey noting the times of the flight and any unusual geophysical or topographic features. Each flight included at least two high elevation 'background' checks. During the high elevation checks, an internal 5 second wide calibration pulse in all EM channels was generated in order to ensure that the gain of the system remained constant and within specifications.

FIELD QA/QC PROCEDURES

On return of the pilot and operator to the base, usually after each flight, the AeroDAS streaming EM and ancillary (magnetic, GPS, radar altimeter) data are carried on removable hard drives and transferred to the data processing work station. At the end of each day, the base station magnetometer data on FlashCard is retrieved from the base station unit.

Data verification and quality control includes a comparison of the acquired GPS data with the flight plan; verification and conversion of the magnetic data to an ASCII format XYZ data file; verification of the base station magnetometer data and conversion to ASCII format XYZ data; and loading, processing and conversion of the steaming EM data from the removable hard drive. All data is then merged to an ASCII XYZ format file which is then imported to an Oasis database for further QA/QC and for the production of preliminary EM, magnetic, and flight path maps.

Survey lines which show excessive deviation from the intended flight path are re-flown. Any line or portion of a line on which the data quality did not meet the contract specification was noted and reflown.

AIRCRAFT AND EQUIPMENT

AIRCRAFT

A Eurocopter (Aerospatiale) AS315B helicopter - registration C-GLOV was used as survey platform. The helicopter was owned and operated by Hiwood Helicopters Ltd. Installation of the geophysical and ancillary equipment was carried out by Aeroquest Limited personnel in conjunction with a licensed aircraft. The survey aircraft was flown at a nominal terrain clearance of 281 ft (86.1metres).

Figure 2 Helicopter of the type used during the survey

MAGNETOMETER

The AeroTEM III airborne survey system employs the Geometrics G-823A caesium vapour magnetometer sensor installed in a two metre towed bird airfoil attached to the main tow line, 38.1 metres above EM bird (Figure 3). The sensitivity of the magnetometer is 0.001 NanoTesla at

a 0.1 second sampling rate. The nominal ground clearance of the magnetometer bird is 68.1 metres (222 ft.). The magnetic data is recorded at 10 Hz by the ADAS.

ELECTROMAGNETIC SYSTEM

The electromagnetic system is an Aeroquest AeroTEM III time domain towed-bird system (Figure 3). The current AeroTEM III transmitter dipole moment is 183 kNIA. The AeroTEM bird is towed 56.1 metres (183 ft) below the helicopter. More technical details of the system may be found in Appendix 5.

The wave-form is triangular with a symmetric transmitter on-time pulse of 1.10 ms and a base frequency of 90 Hz (Figure 4). The current alternates polarity every on-time pulse. During every Tx on-off cycle (180 per second), 200 contiguous channels of raw X and Z component (and a transmitter current monitor, itx) of the received waveform are measured. Each channel width is 27.78 microseconds starting at the beginning of the transmitter pulse. This 200 channel data is referred to as the raw streaming data. The AeroTEM system has one EM data recording streams, the newly designed AeroDAS system which records the full waveform (Figure 4).

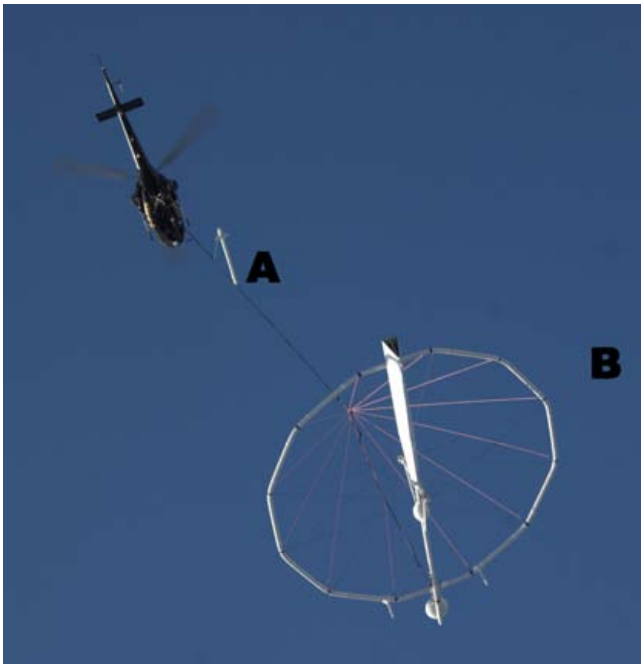

Figure 3. The magnetometer bird (A) and AeroTEM III EM bird (B)

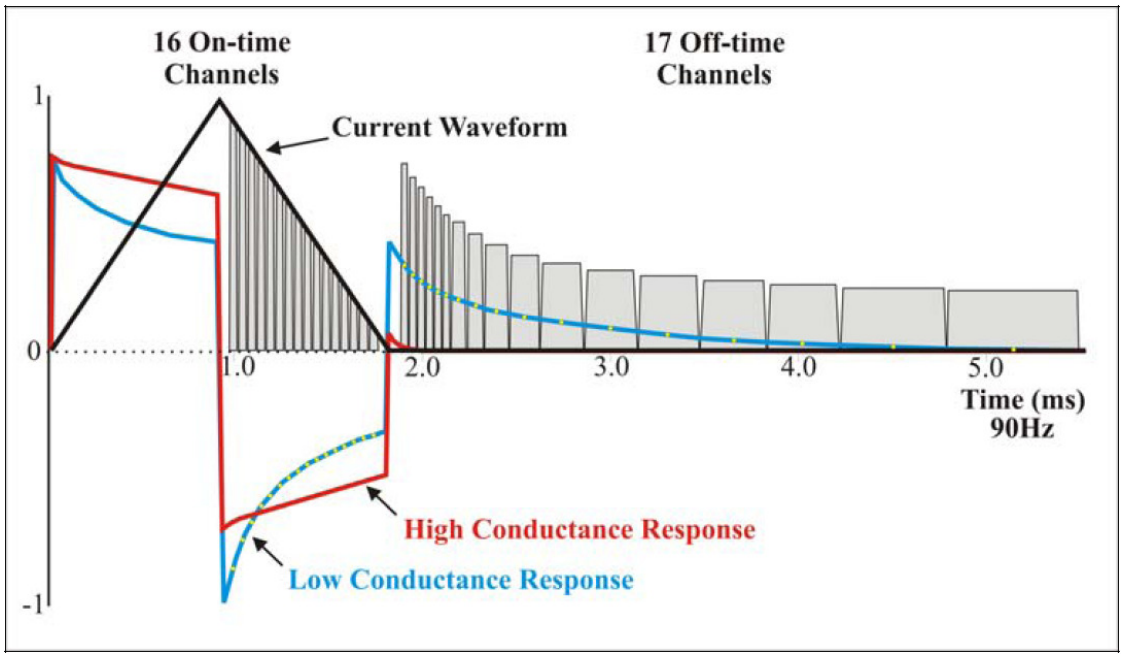

Figure 4. Schematic of Transmitter and Receiver waveforms

AERODAS ACQUISITION SYSTEM

The 200 channels of raw streaming data are recorded by the AeroDAS acquisition system (Figure 5) onto a removable hard drive. In addition the magnetic, altimeter and position data are also recorded in it, six channels of real time processed off-time EM decay in the Z direction and one in the X direction can be viewed on a color monitor on board, these channels are derived by a binning, stacking and filtering procedure on the raw streaming data.

The primary use of the displayed EM data (Z1 to Z6, X1), magnetic and altimeter is to provide for real-time QA/QC on board.

Figure 5. AeroTEM III Instrument Rack

The streaming data are processed post-survey to yield 33 stacked and binned on-time and off-time channels at a 10 Hz sample rate. The timing of the final processed EM channels is described in the following table:

```
Average TxOn      -0.4556 us
Average TxSwitch  896.9034 us
Average TxOff     1726.6724 us
Average TxPeak    440.4787 A

[Channel Data]
```

Channel	Sample Range	Time Width (us)	Time Center (us)	Time After TxOn (us)
On1	5 - 5	27.8	125.0	125.5
On2	6 - 6	27.8	152.8	153.2
On3	7 - 7	27.8	180.6	181.0
On4	8 - 8	27.8	208.3	208.8
On5	9 - 9	27.8	236.1	236.6
On6	10 - 10	27.8	263.9	264.3
On7	11 - 11	27.8	291.7	292.1
On8	12 - 12	27.8	319.4	319.9
On9	13 - 13	27.8	347.2	347.7
On10	14 - 14	27.8	375.0	375.5
On11	15 - 15	27.8	402.8	403.2
On12	16 - 16	27.8	430.6	431.0
On13	17 - 17	27.8	458.3	458.8
On14	18 - 18	27.8	486.1	486.6
On15	19 - 19	27.8	513.9	514.3
On16	20 - 20	27.8	541.7	542.1

Channel	Sample Range	Time Width (us)	Time Center (us)	Time After TxOff (us)
Off0	64 - 64	27.8	1763.9	37.2
Off1	65 - 65	27.8	1791.7	65.0
Off2	66 - 66	27.8	1819.4	92.8
Off3	67 - 67	27.8	1847.2	120.5
Off4	68 - 68	27.8	1875.0	148.3
Off5	69 - 69	27.8	1902.8	176.1
Off6	70 - 72	83.3	1958.3	231.7
Off7	73 - 75	83.3	2041.7	315.0
Off8	76 - 78	83.3	2125.0	398.3
Off9	79 - 81	83.3	2208.3	481.7
Off10	82 - 86	138.9	2319.4	592.8
Off11	87 - 91	138.9	2458.3	731.7
Off12	92 - 98	194.4	2625.0	898.3
Off13	99 - 108	277.8	2861.1	1134.4
Off14	109 - 123	416.7	3208.3	1481.7
Off15	124 - 147	666.7	3750.0	2023.3
Off16	148 - 185	1055.6	4611.1	2884.4

MAGNETOMETER BASE STATION

The base magnetometer was an AQL designed PDA caesium vapour magnetometer system with integrated GPS. Data logging and UTC time synchronisation was carried out within the magnetometer, with the GPS providing the timing signal. The data logging was configured to measure at 2.0 second intervals. Digital recording resolution was 0.1 nT. The sensor was placed on a tripod in an area of low magnetic gradient and free of cultural noise sources. A continuously updated display of the base station values was available for viewing and regularly monitored to ensure acceptable data quality and diurnal variation.

RADAR ALTIMETER

A Terra TRA 3500/TRI-30 radar altimeter is used to record terrain clearance. The antenna was mounted on the outside of the helicopter beneath the cockpit. Therefore, the recorded data reflect

the height of the helicopter above the ground. The Terra altimeter has an altitude accuracy of +/- 1.5 metres.

VIDEO TRACKING AND RECORDING SYSTEM

A high resolution digital colour 8 mm video camera is used to record the helicopter ground flight path along the survey lines. The video is digitally annotated with GPS position and time and can be used to verify ground positioning information and cultural causes of anomalous geophysical responses.

Figure 6. Digital video camera typical mounting location.

GPS NAVIGATION SYSTEM

The navigation system consists of an Ag-Nav Incorporated AG-NAV2 GPS navigation system comprising a PC-based acquisition system, navigation software, a deviation indicator in front of the aircraft pilot to direct the flight, a full screen display with controls in front of the operator, a Mid-Tech RX400p WAAS-enabled GPS receiver mounted on the instrument rack and an antenna mounted on the magnetometer bird. WAAS (Wide Area Augmentation System) consists of approximately 25 ground reference stations positioned across the United States that monitor GPS satellite data. Two master stations located on the east and west coasts collect data from the reference stations and create a GPS correction message. This correction accounts for GPS satellite orbit and clock drift plus signal delays caused by the atmosphere and ionosphere. The corrected differential message is then broadcast through one of two geostationary satellites, or satellites with a fixed position over the equator. The corrected position has a published accuracy of less than 3 metres.

Survey co-ordinates are set up prior to the survey and the information is fed into the airborne navigation system. The co-ordinate system employed in the survey design was WGS84 [World] using the UTM zone 10N projection. The real-time differentially corrected GPS positional data was recorded by AeroDAS system in geodetic coordinates (latitude and longitude using WGS84) at 0.2 s intervals.

DIGITAL ACQUISITION SYSTEM

The AeroTEM received waveform sampled during on and off-time at 200 channels per decay, 180 times per second, was logged by the proprietary AeroDAS data acquisition system. The channel sampling commences at the start of the Tx cycle and the width of each channel is 27.78 seconds. In addition the positional and secondary geophysical data, (i.e. magnetic, radar altimeter,

GPS position, and UTC time) was recorded on a removable hard-drive and later backed-up onto DVD-ROM from the field-processing computer.

PERSONNEL

The following Aeroquest personnel were involved in the project:

Project Manager of Operations: Lee Harper
Field Data Processors: Josh Poirier
Field Operator: Viktor Shevchenko
Data Processing and Reporting: Chris Kahue and Asif Mirza

The survey pilot, Chad Goddyn, was employed directly by the helicopter operator – HiWood Helicopters Ltd.

DELIVERABLES

HARDCOPY DELIVERABLES

The report includes two sets of three 1:20,000 maps and the following three geophysical data products are delivered:

TMI – Total Magnetic Intensity (TMI) colour grid with contours and EM anomaly symbols.
ZOFF1– AeroTEM Z1 Off-time colour grid with contours and EM anomaly symbols.
EM – AeroTEM off-time profiles Z3-Z13 and EM anomaly symbols.

The coordinate/projection system for the maps is NAD83 – UTM Zone 9N. For reference, the latitude and longitude in WGS84 are also noted on the maps.

All the maps show flight path trace, skeletal topography, and conductor picks represented by an anomaly symbol classified according to calculated off-time conductance. The anomaly symbol is accompanied by postings denoting the calculated off-time conductance, a thick or thin classification and an anomaly identifier label. The anomaly symbol legend and survey specifications are displayed on the left margin of the maps.

DIGITAL DELIVERABLES

Final Database of Survey Data (.GDB)

The geophysical profile data is archived digitally in a Geosoft GDB binary format databases. A description of the contents of the individual channels in the database can be found in Appendix 2. A copy of this digital data is archived at the Aeroquest head office in Mississauga.

Geosoft Grid files (.GRD)

Levelled Grid products used to generate the geophysical map images. All grids have 20 m cell size.

- Total Magnetic Intensity from Mag sensor on the tow cable (*Berg_TMI.grd*)
- AeroTEM Z Off time Channel 1 *(Berg_Zoff1.grd*)
- Digital Terrain Model (*Berg_DTM.grd*)

Digital Versions of Final Maps (.MAP, .PDF)

Map files in Geosoft .map and Adobe PDF format.

Google Earth Files (.kmz)

Flight navigation lines, EM Anomalies and geophysical grids in Google earth kmz format. Double click to view in Google Earth.

Free Viewing Software (.EXE)

Geosoft Oasis Montaj Viewing Software
Adobe Acrobat Reader
Google Earth Viewer

Digital Copy of this Document (.PDF)

Adobe PDF format of this document.

DATA PROCESSING AND PRESENTATION

All in-field and post-field data processing was carried out using Aeroquest proprietary data processing software and Geosoft Oasis Montaj software. Maps were generated using 36-inch and 42-inch wide Hewlett Packard ink-jet plotters.

BASE MAP

The geophysical maps accompanying this report are based on positioning in the NAF83 datum. The survey geodetic GPS positions have been projected using the Universal Transverse Mercator projection in Zone 9 North. A summary of the map datum and projection specifications is given following:

Ellipse: GRS 1980
Ellipse major axis: 6378137m eccentricity: 0.081819191
Datum: North American 1983 - Canada Mean
Datum Shifts (x,y,z) : 0, 0, 0 metres
Map Projection: Universal Transverse Mercator Zone 9 (Central Meridian 123ºW)
Central Scale Factor: 0.9996
False Easting, Northing: 500,000m, 0m

The background vector topography was sourced from client at 1:20000 scale and the background shading were derived from NASA Shuttle Radar Topography Mission (SRTM) 90 metre resolution DEM data.

FLIGHT PATH & TERRAIN CLEARANCE

The position of the survey helicopter was directed by use of the Global Positioning System (GPS). Positions were updated five times per second (5 Hz) and expressed as WGS84 latitude and longitude calculated from the raw pseudo range derived from the C/A code signal. The instantaneous GPS flight path, after conversion to UTM co-ordinates, is drawn using linear interpolation between the x/y positions. The terrain clearance was maintained with reference to the radar altimeter. The raw Digital Terrain Model (DTM) was derived by taking the GPS survey

elevation and subtracting the radar altimeter terrain clearance values. The calculated topography elevation values are relative and are not tied in to surveyed geodetic heights.

Each flight included at least two high elevation 'background' checks. These high elevation checks are to ensure that the gain of the system remained constant and within specifications.

ELECTROMAGNETIC DATA

The raw streaming data, sampled at a rate of 36,000 Hz (200 channels, 180 times per second) was reprocessed using a proprietary software algorithm developed and owned by Aeroquest Limited. Processing involves the compensation of the X and Z component data for the primary field waveform. Coefficients for this compensation for the system transient are determined and applied to the stream data. The stream data are then pre-filtered, stacked, binned to the 33 on and off-time channels and checked for the effectiveness of the compensation and stacking processes. The stacked data is then filtered, levelled and split up into the individual line segments. Further base level adjustments may be carried out at this stage. The filtering of the stacked data is designed to remove or minimize high frequency noise that cannot be sourced from the geology.

The final field processing step was to merge the processed EM data with the other data sets into a Geosoft GDB file. The EM fiducial is used to synchronize the two datasets. The processed channels are merged into 'array format; channels in the final Geosoft database as Zon, Zoff, Xon, and Xoff.

Apparent bedrock EM anomalies were interpreted with the aid of an auto-pick from positive peaks and troughs in the off-time Z channel responses correlated with X channel responses. The auto-picked anomalies were reviewed and edited by a geophysicist on a line by line basis to discriminate between thin and thick conductor types. Anomaly picks locations were migrated and removed as required. This process ensures the optimal representation of the conductor centres on the maps.

At each conductor pick, estimates of the off-time conductance have been generated based on a horizontal plate source model for those data points along the line where the response amplitude is sufficient to yield an acceptable estimate. Some of the EM anomaly picks do not display a Tau value; this is due to the inability to properly define the decay of the conductor usually because of low signal amplitudes. Each conductor pick was then classified according to a set of seven ranges of calculated off-time conductance values. For high conductance sources, the on-time conductance values may be used, since it provides a more accurate measure of high-conductance sources. Each symbol is also given an identification letter label, unique to each flight line. Conductor picks that did not yield an acceptable estimate of off-time conductance due to a low amplitude response were classified as a low conductance source. Please refer to the anomaly symbol legend located in the margin of the maps.

MAGNETIC DATA

Prior to any levelling the magnetic data was subjected to a lag correction of -0.1 seconds and a spike removal filter. The filtered aeromagnetic data were then corrected for diurnal variations using the magnetic base station and the intersections of the tie lines. No corrections for the regional reference field (IGRF) were applied. The corrected profile data were interpolated on to a grid using a bi-directional grid technique with a grid cell size of 40 metres.

GENERAL COMMENTS

The survey was successful in mapping the magnetic and conductive properties of the geology throughout the survey area. Below is a brief interpretation of the results. For a detailed interpretation please contact Aeroquest Limited.

MAGNETIC RESPONSE

The magnetic data provide a high resolution map of the distribution of the magnetic mineral content of the survey area. This data can be used to interpret the location of geological contacts and other structural features such as faults and zones of magnetic alteration. The sources for anomalous magnetic responses are generally thought to be predominantly magnetite because of the relative abundance and strength of response (high magnetic susceptibility) of magnetite over other magnetic minerals such as pyrrhotite.

EM ANOMALIES

The EM anomalies on the maps are classified by conductance (as described earlier in the report) and also by the thickness of the source. A thin, vertically orientated source produces a double peak anomaly in the z-component response and a positive to negative crossover in the x-component response (Figure 7). For a vertically orientated thick source (say, greater than 10 metres), the response is a single peak in the z-component response and a negative to positive crossover in the x-component response (Figure 8). Because of these differing responses, the AeroTEM system provides discrimination of thin and thick sources and this distinction is indicated on the EM anomaly symbols (N = thin and K = thick). Where multiple, closely spaced conductive sources occur, or where the source has a shallow dip, it can be difficult to uniquely determine the type (thick vs. thin) of the source (Figure 9). In these cases both possible source types may be indicated by picking both thick and thin response styles. For shallow dipping conductors the 'thin' pick will be located over the edge of the source, whereas the 'thick' pick will fall over the downdip 'heart' of the anomaly.

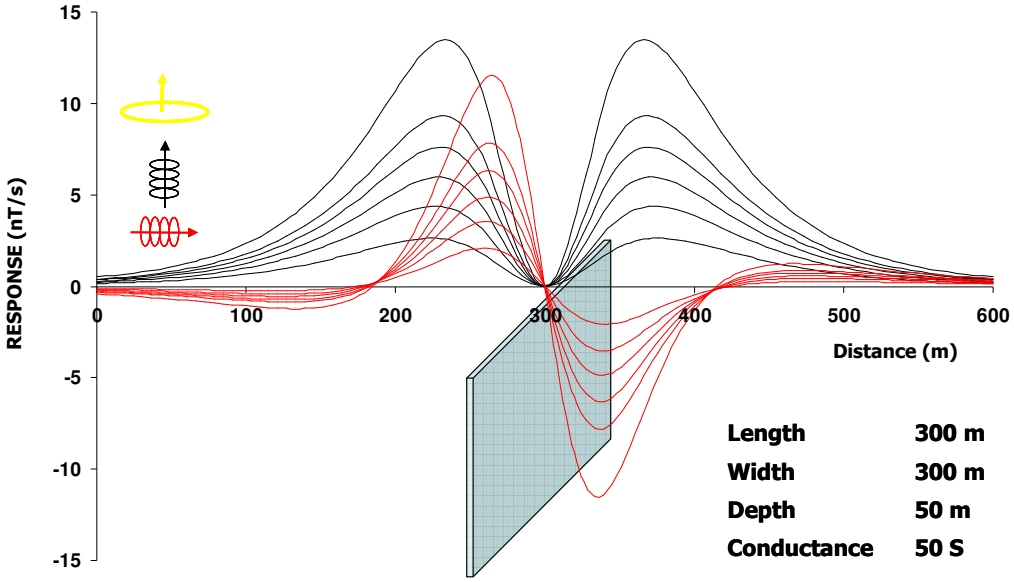

Figure 7. AeroTEM response to a 'thin' vertical conductor.

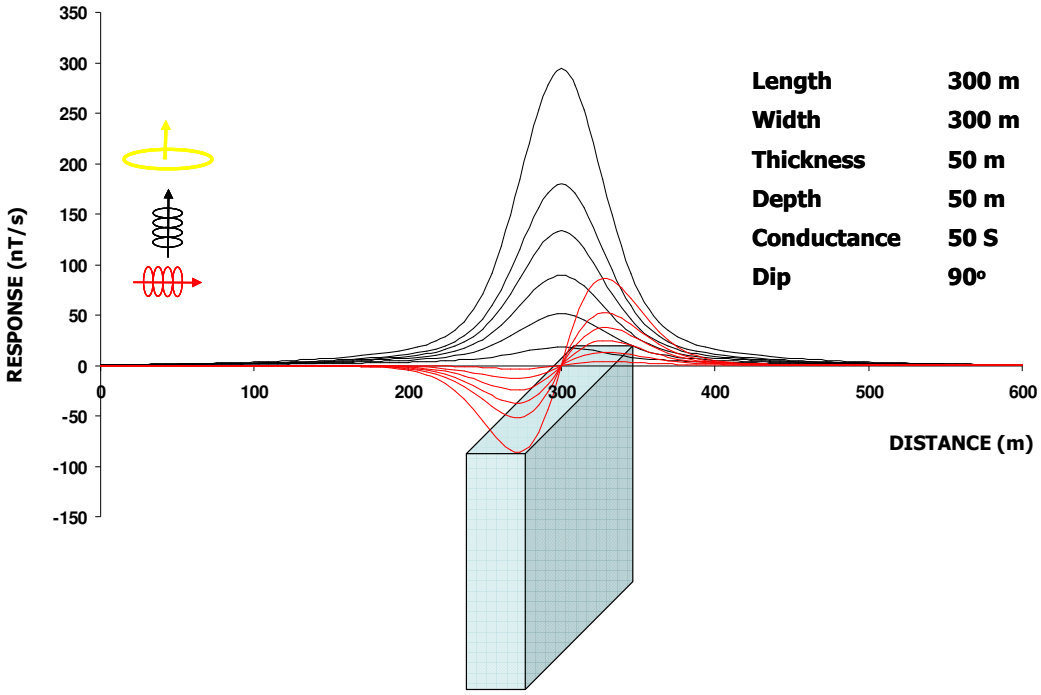

Figure 8. AeroTEM response for a 'thick' vertical conductor.

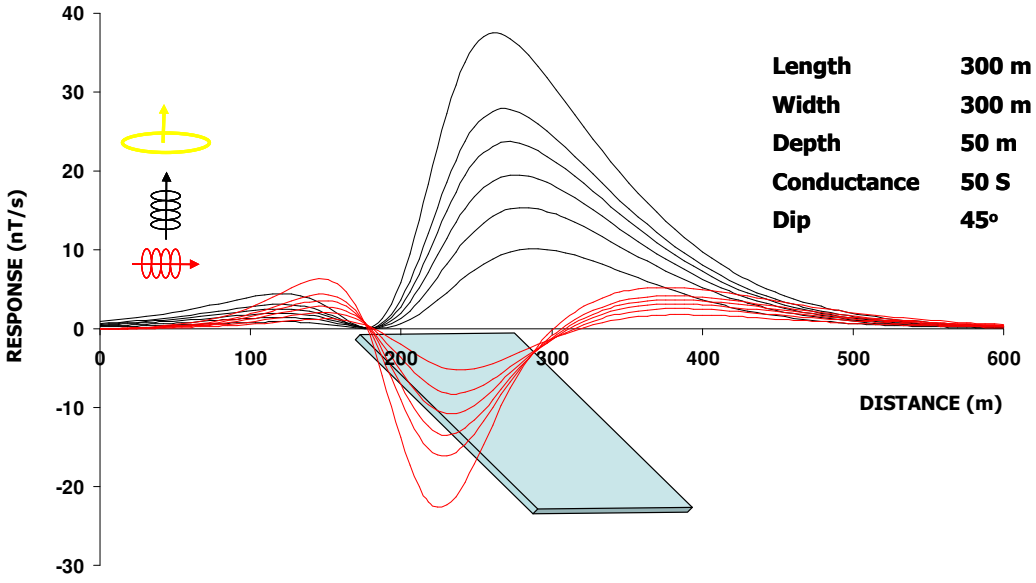

Figure 9. AeroTEM response over a 'thin' dipping conductor.

All cases should be considered when analyzing the interpreted picks and prioritizing for follow-up. Specific anomalous responses which remain as high priority should be subjected to numerical modeling prior to drill testing to determine the dip, depth and probable geometry of the source.

APPENDIX 1: SURVEY BOUNDARIES

The following table presents the Berg boundary. All geophysical data presented in this report have been windowed to 100m outside of these boundaries. X and Y positions are in metres: NAD83 UTM Zone 9N.

Berg Block:

X	Y
600181.8	5968299.3
616405.4	5968299.3
616405.4	5960106.5
600181.8	5960106.5

APPENDIX 2: DESCRIPTION OF DATABASE FIELDS

The GDB's files are a Geosoft binary database. In the each database, the Survey lines and Tie Lines are prefixed with an "L" for "Line" and "T" for "Tie".

database: (*10-044_Berg.gdb*).

COLUMN	UNITS	DESCRIPTOR
Line		Line number
Flight		Flight #
Emfid		AERODAS Fiducial
utctime	hh:mm:ss.ss	UTC time
X	m	UTM Easting (NAD83, Zone 09)
Y	m	UTM Northing (NAD83, Zone 09)
Galt	m	GPS elevation of magnetometer bird
Ralt	m	Helicopter radar altimeter (height above terrain)
bheight	m	Terrain clearance of EM bird
basemag	nT	Base station total magnetic intensity
magU	nT	Final levelled total magnetic intensity from magnetometer sensor
Dtm	m	Digital Terrain Model
Zon	nT/s	EM On-Time Z component Channels 1-16
Zoff	nT/s	EM Off-Time Z component Channels 0-16
Xon	nT/s	EM On-Time X component Channels 1-16
Xoff	nT/s	EM Off-Time X component Channels 0-16
pwrline		powerline monitor data channel
Grade		Classification from 1-7 based on conductance of conductor pick
Anom_Labels		Letter label of conductor pick (Unique per flight line)
Off_Con	S	Off-time conductance at conductor pick
Off_Tau	µs	Off-time decay constant at conductor pick
Anom_ID		EM Anomaly response style (K= thicK, N = thiN)
Off_AllCon	S	Off-time conductance
Off_AllTau	µs	Off-time decay constant
TranOff	µs	Transmitter turn off time
TranOn	µs	Transmitter turn on time
TranPeak	A	Transmitter peak current
TranSwitch	µs	Transmitter peak current time
Off_Pick		Anomaly pick channel

APPENDIX 3: AEROTEM ANOMALY LISTING

Berg Block

Line	Anom	ID	Cond (S)	Tau (µs)	Flight #	UTC Time	Bird height (m)	Easting (m)	Northing (m)
10025	A	K	0.1	38.0	31	0:24:51	61.9	604790.7	5968007.1
10025	B	K	1.6	126.2	31	0:26:29	48.1	606954.9	5967993.9
10025	C	N	1.3	112.7	31	0:30:40	52.8	610169.5	5967995.3
10025	D	K	3.9	197.6	31	0:31:39	43.6	611404.8	5967990.5
10025	E	N	0.8	87.1	31	0:33:53	41.6	614467.3	5967990.2
10035	A	N	0.4	60.5	31	0:37:45	54.0	614511.8	5967794.0
10035	B	K	1.6	126.1	31	0:39:38	49.8	611421.4	5967812.0
10035	C	N	1.5	121.1	31	0:40:30	53.7	610154.5	5967813.4
10035	A	K	1.1	103.9	31	0:46:39	38.3	606970.7	5967828.4
10035	B	K	0.4	60.0	31	0:48:30	73.9	604870.6	5967807.2
10045	A	K	0.4	64.9	31	1:03:49	62.0	604870.2	5967580.8
10045	B	K	0.2	45.5	31	1:05:50	42.3	606946.6	5967587.6
10045	C	N	0.2	48.9	31	1:06:32	49.1	607631.6	5967596.2
10045	D	N	0.3	58.4	31	1:09:40	75.5	610103.9	5967606.1
10045	E	K	1.9	139.4	31	1:10:55	51.8	611453.9	5967589.1
10045	F	K	0.2	44.8	31	1:12:30	37.9	613630.2	5967604.9
10045	G	N	0.4	59.3	31	1:13:07	50.9	614507.3	5967597.4
10050	A	K	*	*	7	16:39:01	35.1	615941.0	5967406.9
10050	B	N	0.6	76.4	7	16:39:57	36.5	614553.0	5967400.9
10050	C	K	0.1	37.4	7	16:40:28	36.8	613752.0	5967390.2
10050	D	K	0.3	55.4	7	16:41:42	46.0	611714.3	5967401.8
10050	A	N	0.2	43.7	7	16:46:50	50.1	607691.2	5967409.8
10060	A	K	0.1	33.5	8	19:01:14	39.8	615811.7	5967190.7
10060	B	N	0.6	78.6	8	19:02:03	31.1	614632.0	5967206.0
10060	C	K	0.5	71.8	8	19:02:38	38.9	613800.1	5967204.7
10060	D	K	0.3	52.4	8	19:03:56	52.9	611769.7	5967186.1
10060	E	N	0.3	52.4	8	19:08:38	49.6	607708.8	5967216.2
10060	A	K	0.4	61.9	8	19:18:40	127.9	604819.8	5967210.9
10060	A	K	0.1	29.7	8	19:13:20	40.5	606265.4	5967193.0
10070	A	K	0.1	37.9	14	18:40:19	25.7	615658.4	5967004.8
10070	B	K	0.6	79.4	14	18:40:59	29.7	614707.9	5967000.1
10070	C	K	0.7	86.3	14	18:41:39	39.4	613788.0	5967007.1
10070	D	K	0.2	44.3	14	18:45:07	44.0	609731.3	5966998.9
10070	E	N	0.2	44.3	14	18:47:17	48.8	607818.7	5967002.0
10070	F	K	0.1	26.0	14	18:49:42	42.4	606231.5	5966991.1

Line	Anom	ID	Cond (S)	Tau (µs)	Flight #	UTC Time	Bird height (m)	Easting (m)	Northing (m)
10080	A	K	0.1	33.5	14	19:08:59	55.9	606118.9	5966799.8
10080	B	K	0.1	23.8	14	19:11:22	52.6	608556.1	5966797.5
10080	C	K	0.3	56.7	14	19:13:31	73.8	609792.1	5966787.0
10080	D	N	0.3	56.7	14	19:14:55	52.4	611031.0	5966793.0
10080	E	K	1.2	107.1	14	19:17:03	34.1	613841.1	5966798.9
10080	F	K	0.6	76.7	14	19:17:52	27.6	615106.8	5966812.0
10080	G	K	0.8	91.9	14	19:18:06	56.0	615469.2	5966818.8
10090	A	K	1.3	114.2	15	20:36:18	49.7	614949.8	5966622.7
10090	B	K	1.3	115.3	15	20:37:04	41.8	613881.4	5966605.6
10090	C	N	0.3	53.6	15	20:39:08	49.2	610929.2	5966602.5
10090	D	K	0.6	74.8	15	20:40:11	61.8	609861.5	5966621.2
10090	E	K	0.1	32.8	15	20:41:26	61.6	608548.9	5966601.2
10100	A	K	0.1	27.4	15	21:06:39	63.8	608560.1	5966397.1
10100	B	K	0.9	96.6	15	21:07:39	55.6	609711.9	5966404.1
10100	C	N	0.1	38.0	15	21:08:29	61.0	610918.3	5966409.5
10100	D	K	1.0	99.8	15	21:10:35	43.2	613861.6	5966410.1
10110	A	K	1.6	126.1	16	2:29:27	34.8	615089.6	5966204.7
10110	B	K	1.6	126.7	16	2:30:26	42.3	613855.4	5966213.7
10110	C	K	0.4	64.4	16	2:34:18	52.8	609787.0	5966213.7
10120	A	K	1.3	111.6	16	3:06:12	47.4	609829.8	5966008.9
10120	B	K	1.2	110.3	16	3:09:58	66.1	613480.4	5966002.0
10120	C	K	1.2	110.5	16	3:10:31	46.3	614166.2	5966014.4
10120	D	K	0.4	65.4	16	3:11:22	46.1	615209.5	5965989.8
10130	A	K	0.3	49.6	17	16:01:43	32.6	615314.3	5965803.3
10130	B	N	0.4	58.9	17	16:03:35	25.4	613329.2	5965803.2
10130	C	K	0.9	96.2	17	16:07:33	50.7	609842.2	5965796.4
10140	A	K	0.1	32.3	17	16:32:52	33.3	606150.2	5965606.7
10141	A	K	0.9	96.2	18	16:49:26	34.0	609782.3	5965597.8
10141	B	N	0.1	26.6	18	16:53:03	62.2	613251.0	5965577.6
10141	C	K	0.3	56.7	18	16:55:15	51.6	615340.8	5965595.3
10150	A	K	0.2	48.4	19	18:02:29	44.9	615299.9	5965411.2
10150	B	N	0.2	48.4	19	18:03:48	38.5	613812.7	5965411.4
10150	C	N	0.2	48.4	19	18:04:44	19.1	613219.2	5965411.9
10150	D	K	0.4	64.1	19	18:08:10	47.4	610734.7	5965392.5
10150	E	K	0.4	66.6	19	18:08:49	33.6	609981.8	5965400.7
10150	F	N	2.2	148.3	19	18:09:06	45.3	609680.3	5965397.1
10150	G	K	0.2	40.5	19	18:13:41	46.2	606045.0	5965403.4
10161	A	K	14.1	375.2	20	18:44:41	39.1	609351.4	5965196.5
10161	B	N	4.5	212.7	20	18:45:07	35.8	609772.4	5965178.3

Line	Anom	ID	Cond (S)	Tau (µs)	Flight #	UTC Time	Bird height (m)	Easting (m)	Northing (m)
10161	C	K	1.8	132.5	20	18:46:05	54.2	610725.5	5965192.0
10161	D	N	1.0	99.2	20	18:51:02	62.3	613690.8	5965222.8
10161	E	K	1.0	99.2	20	18:53:24	43.1	616343.8	5965197.5
10170	A	K	0.8	90.5	21	19:51:19	49.0	616471.2	5964998.6
10170	B	N	0.3	50.3	21	19:54:00	31.9	613689.1	5965000.1
10170	C	K	7.5	274.4	21	19:58:32	31.8	610682.7	5965002.0
10170	D	K	19.5	441.6	21	20:00:14	58.7	609242.0	5965015.2
10180	A	K	12.6	354.8	21	20:27:50	58.3	609186.8	5964804.4
10180	B	K	13.9	373.1	21	20:30:00	58.5	610686.9	5964806.4
10180	C	N	0.2	48.6	21	20:35:11	27.2	613623.8	5964797.1
10190	A	K	8.0	283.5	22	21:49:38	38.5	610772.0	5964613.8
10190	B	K	8.5	292.3	22	21:52:24	52.9	609076.8	5964628.0
10190	A	K	0.6	74.4	22	21:57:20	41.5	604804.0	5964610.6
10201	A	K	1.8	133.3	23	0:07:37	45.1	610792.2	5964418.4
10201	B	K	1.5	123.2	23	0:10:30	56.9	608968.4	5964415.2
10210	A	K	0.4	65.3	23	0:29:32	44.2	603343.2	5964191.7
10210	B	N	0.4	63.2	23	0:35:42	54.2	608578.1	5964191.3
10210	C	K	1.4	119.4	23	0:35:56	43.2	608887.2	5964194.8
10210	D	K	1.5	121.5	23	0:38:31	45.2	610872.3	5964226.5
10220	A	K	0.5	67.0	24	1:39:28	47.7	611035.8	5964011.0
10220	B	K	1.5	123.6	24	1:43:16	39.6	608786.6	5964010.8
10220	C	K	0.8	87.1	24	1:50:12	97.8	603321.6	5964017.9
10230	A	K	1.5	123.7	24	2:01:12	48.2	603189.7	5963805.3
10230	B	K	1.2	107.5	24	2:02:04	51.2	603584.7	5963798.3
10230	C	K	1.8	132.6	24	2:07:18	47.3	608726.9	5963809.4
10230	D	K	0.4	59.1	24	2:10:17	57.0	611092.7	5963805.9
10230	E	K	0.7	80.9	24	2:13:41	52.6	612731.6	5963811.6
10230	F	K	0.5	67.0	24	2:16:03	59.6	614944.2	5963800.9
10240	A	K	0.9	95.8	25	16:28:27	45.8	612823.8	5963589.7
10240	B	K	0.5	73.6	25	16:30:39	54.2	611187.3	5963586.0
10240	C	N	0.5	73.6	25	16:31:05	21.2	610778.1	5963611.4
10240	D	K	3.2	179.3	25	16:37:13	83.9	608743.5	5963611.5
10240	E	K	0.7	83.2	25	16:37:36	53.5	608341.7	5963605.3
10240	F	K	2.1	145.8	25	16:44:23	82.0	603510.0	5963576.6
10240	G	K	13.4	365.5	25	16:44:35	38.7	603311.6	5963580.3
10250	A	K	7.2	268.1	25	16:56:25	50.6	603193.9	5963408.0
10250	B	K	1.7	130.3	25	16:56:59	55.9	603687.4	5963398.3
10250	C	K	1.1	106.5	25	17:04:29	37.0	608391.8	5963408.7
10250	D	K	10.4	321.7	25	17:04:50	50.5	608729.7	5963397.5

Line	Anom	ID	Cond (S)	Tau (µs)	Flight #	UTC Time	Bird height (m)	Easting (m)	Northing (m)
10250	E	K	0.3	51.7	25	17:09:11	34.8	611142.2	5963405.0
10250	A	K	0.4	64.0	25	17:20:24	55.5	612997.2	5963385.5
10260	A	K	0.9	93.3	26	18:57:05	92.4	612988.0	5963199.5
10260	B	K	0.4	61.2	26	19:00:13	45.9	611148.8	5963198.0
10260	C	K	3.4	185.2	26	19:06:42	64.5	608644.0	5963218.6
10260	D	N	7.3	270.9	26	19:07:07	38.0	608210.5	5963203.9
10260	E	K	4.0	199.6	26	19:13:16	82.6	603748.1	5963198.7
10260	F	K	10.8	329.1	26	19:13:53	52.3	603193.7	5963190.4
10260	G	K	2.6	160.6	26	19:14:12	39.7	602865.7	5963173.0
10270	A	K	2.6	162.2	26	19:23:21	45.2	602652.1	5963004.3
10270	A	K	5.5	235.0	26	19:26:39	55.7	603776.9	5962986.6
10270	B	K	2.6	160.2	26	19:32:15	52.1	608471.0	5962991.4
10270	C	K	0.4	64.2	26	19:36:48	46.4	611221.4	5963011.0
10270	D	K	0.9	94.8	26	19:37:09	34.5	611569.6	5963005.6
10270	E	K	0.9	95.1	26	19:39:50	63.1	612943.7	5963002.5
10282	A	K	0.8	91.9	27	21:08:24	49.4	612840.0	5962791.8
10282	B	K	0.9	92.9	27	21:10:30	53.6	611679.0	5962795.3
10282	C	K	0.6	78.1	27	21:10:56	47.0	611229.7	5962807.5
10282	D	K	1.1	106.2	27	21:15:58	59.6	608436.0	5962816.0
10282	E	N	0.1	30.5	27	21:16:35	46.6	607642.5	5962779.6
10282	F	K	9.5	308.2	27	21:20:42	100.1	603758.4	5962815.9
10282	G	K	4.1	202.2	27	21:21:47	45.3	602512.3	5962787.7
10290	A	K	5.2	227.1	28	22:48:21	34.7	613242.0	5962605.6
10290	B	K	1.9	138.6	28	22:49:00	41.1	612804.9	5962589.0
10290	C	K	1.0	99.5	28	22:50:23	42.9	611792.1	5962606.4
10290	D	K	0.9	93.0	28	22:50:53	38.5	611329.5	5962607.5
10290	E	K	3.5	186.1	28	22:57:29	58.2	608607.3	5962595.1
10290	F	K	1.7	130.3	28	22:58:04	47.2	608192.1	5962603.2
10290	G	N	0.1	32.2	28	22:58:35	48.0	607637.6	5962591.7
10290	H	K	3.6	190.1	28	23:06:27	72.3	603776.5	5962600.4
10290	I	K	6.8	259.8	28	23:08:45	37.3	602631.8	5962566.3
10290	J	K	0.6	76.8	28	23:09:32	43.4	601776.7	5962599.1
10300	A	K	4.2	205.1	28	23:14:40	37.9	602560.1	5962393.0
10300	B	K	2.2	148.1	28	23:16:52	34.3	603700.2	5962400.3
10300	C	N	2.4	156.0	28	23:22:48	42.4	607920.6	5962415.0
10300	D	K	1.1	105.5	28	23:23:26	27.9	608558.1	5962405.4
10300	E	K	1.3	111.8	28	23:29:29	48.3	611459.3	5962404.8
10300	F	K	1.0	100.2	28	23:29:52	40.2	611905.0	5962406.8
10300	G	K	0.9	95.1	28	23:30:40	72.4	612677.6	5962380.4

Line	Anom	ID	Cond (S)	Tau (µs)	Flight #	UTC Time	Bird height (m)	Easting (m)	Northing (m)
10300	H	K	0.5	70.3	28	23:31:38	45.1	613772.1	5962409.4
10310	A	K	5.6	235.6	13	17:13:30	31.2	602478.6	5962197.4
10310	B	K	2.5	157.5	13	17:13:52	32.8	602892.4	5962202.2
10310	C	K	8.6	293.0	13	17:20:28	42.2	607792.9	5962222.7
10310	D	K	3.0	173.3	13	17:21:25	50.1	608481.9	5962198.4
10310	E	K	1.1	104.4	13	17:26:40	36.6	611673.6	5962216.5
10310	F	K	1.4	116.2	13	17:26:57	39.7	611994.4	5962206.4
10310	G	K	1.5	122.6	13	17:27:56	39.6	612670.4	5962207.8
10310	H	K	0.7	84.1	13	17:28:56	46.3	613690.3	5962192.4
10320	A	K	1.1	104.2	13	16:47:27	44.6	613536.3	5962016.2
10320	B	K	1.1	106.3	13	16:48:43	74.2	612632.6	5961993.7
10320	C	N	1.7	130.6	13	16:54:38	91.2	608372.9	5962016.7
10320	D	K	6.3	250.2	13	16:55:10	43.3	607832.5	5962009.4
10320	E	K	5.0	223.6	13	17:04:54	33.7	602923.3	5962016.5
10320	F	K	7.0	263.9	13	17:05:14	46.3	602588.9	5962027.6
10330	A	K	6.0	245.1	12	2:50:00	62.3	602679.8	5961815.7
10330	B	K	3.0	174.4	12	2:56:59	48.1	607708.4	5961794.5
10330	C	N	0.6	78.3	12	2:57:30	49.6	608313.1	5961801.3
10330	D	K	3.4	184.6	12	3:05:17	47.4	612738.6	5961807.4
10330	E	K	0.6	75.6	12	3:06:09	61.4	613513.2	5961772.3
10340	A	N	0.7	80.7	12	2:26:51	40.3	613586.7	5961599.8
10340	B	K	1.4	118.3	12	2:27:56	46.0	612664.6	5961596.5
10340	C	N	0.9	96.4	12	2:34:32	69.5	608232.0	5961599.8
10340	D	N	0.9	96.4	12	2:35:15	39.8	607384.0	5961596.6
10340	E	K	0.5	68.7	12	2:40:39	41.5	603479.9	5961595.4
10340	F	K	0.8	86.3	12	2:41:17	46.3	602718.9	5961611.4
10350	A	K	0.3	57.1	11	1:24:46	42.7	602885.3	5961408.8
10350	B	N	0.7	82.8	11	1:30:26	40.6	608171.1	5961418.9
10350	C	N	0.2	48.8	11	1:30:49	28.3	608491.9	5961405.3
10350	D	K	0.7	81.8	11	1:37:30	47.8	613609.9	5961413.4
10365	A	N	0.9	96.4	32	2:55:10	42.5	608119.5	5961198.1
10365	B	N	1.0	101.5	32	2:55:30	36.5	608466.2	5961192.6
10370	A	N	0.8	89.7	10	23:52:31	43.0	607377.1	5960983.8
10370	B	N	0.6	78.1	10	23:53:03	47.1	608049.7	5961011.2
10370	C	N	1.4	119.9	10	23:53:23	36.1	608511.6	5961016.5
10380	A	K	2.3	151.9	10	23:30:27	50.0	608245.2	5960823.9
10380	B	K	1.1	105.6	10	23:32:39	40.4	605964.2	5960808.9
10380	A	K	0.0	20.0	10	23:36:35	29.7	604890.7	5960804.7
10390	A	K	0.1	26.1	9	21:40:39	41.2	603730.1	5960601.3

Line	Anom	ID	Cond (S)	Tau (µs)	Flight #	UTC Time	Bird height (m)	Easting (m)	Northing (m)
10390	B	K	0.6	78.7	9	21:42:54	55.3	605864.2	5960618.1
10390	C	N	0.5	72.0	9	21:43:59	57.0	607195.3	5960581.2
10390	D	K	0.9	96.5	9	21:44:45	60.0	608147.9	5960613.7
10400	A	K	4.3	207.0	9	21:21:15	35.0	608013.1	5960408.6
10400	B	N	0.8	90.1	9	21:21:55	55.4	607228.1	5960423.8
10400	C	K	0.2	38.7	9	21:23:57	67.0	605736.1	5960404.5
10400	D	K	1.4	118.2	9	21:24:46	55.4	604706.4	5960398.9
10400	E	K	0.1	31.3	9	21:26:12	64.8	603804.7	5960397.5
10410	A	N	1.1	106.2	7	17:48:46	41.4	607218.1	5960192.7
10410	B	K	15.9	398.1	7	17:49:21	29.0	607726.4	5960209.2
10410	C	K	3.6	190.3	7	17:49:32	32.4	607907.1	5960212.2
10410	A	K	0.2	39.4	7	17:41:46	56.1	603855.7	5960189.7
10410	B	K	2.8	166.4	7	17:43:06	114.9	604655.4	5960202.3
19025	A	N	20.0	447.3	32	2:30:06	47.2	602290.5	5962463.3
19040	A	K	0.0	20.6	4	21:40:53	30.0	606273.2	5967138.6
19040	B	K	0.1	34.2	4	21:42:19	28.5	606268.9	5965582.2
19040	C	K	1.7	129.3	4	21:47:26	50.1	606278.2	5960946.3
19050	A	K	2.5	156.8	4	21:31:17	41.4	608279.9	5960858.9
19050	B	K	2.8	167.7	4	21:31:37	38.3	608285.3	5961352.2
19050	C	K	2.6	160.4	4	21:32:25	53.6	608294.6	5962628.6
19060	A	K	1.3	115.2	4	21:22:26	38.1	610284.7	5965143.1
19070	A	K	1.3	112.1	4	21:08:26	65.4	612272.3	5961988.9
19070	B	K	2.2	149.2	4	21:09:23	46.3	612284.6	5962438.9
19080	A	K	0.5	73.1	4	20:51:55	45.0	614298.7	5967056.0
19090	A	K	0.9	96.9	4	20:46:05	44.0	616281.5	5965120.3

APPENDIX 4: AEROTEM DESIGN CONSIDERATIONS

Helicopter-borne EM systems offer an advantage that cannot be matched from a fixed-wing platform. The ability to fly at slower speed and collect dat

3a with high spatial resolution, and with great accuracy, means the helicopter EM systems provide more detail than any other EM configuration, airborne or ground-based. Spatial resolution is especially important in areas of complex geology and in the search for discrete conductors. With the advent of helicopter-borne high-moment time domain EM systems the fixed wing platforms are losing their *only* advantage – depth penetration.

Advantage 1 – Spatial Resolution

The AeroTEM system is specifically designed to have a small footprint. This is accomplished through the use of concentric transmitter-receiver coils and a relatively small diameter transmitter coil (5 m). The result is a highly focused exploration footprint, which allows for more accurate "mapping" of discrete conductors. Consider the transmitter primary field images shown in Figure 1, for AeroTEM versus a fixed-wing transmitter.

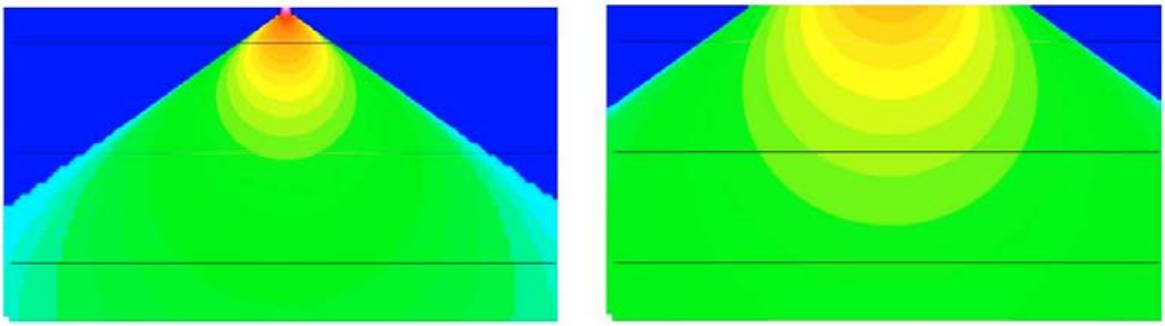

The footprint of AeroTEM at the earth's surface is roughly 50m on either side of transmitter

The footprint of a fixed-wing system is roughly 150 m on either side of the transmitter

Figure 1. A comparison of the footprint between AeroTEM and a fixed-wing system, highlights the greater resolution that is achievable with a transmitter located closer to the earth's surface. The AeroTEM footprint is one third that of a fixed-wing system and is symmetric, while the fixed-wing system has even lower spatial resolution along the flight line because of the separated transmitter and receiver configuration.

At first glance one may want to believe that a transmitter footprint that is distributed more evenly over a larger area is of benefit in mineral exploration. In fact, the opposite is true; by energizing a larger surface area, the ability to energize and detect discrete conductors is reduced. Consider, for example, a comparison between AeroTEM and a fixed-wing system over the Mesamax Deposit (1,450,000 tonnes of 2.1% Ni, 2.7% Cu, 5.2 g/t Pt/Pd). In a test survey over three flight lines spaced 100 m apart, AeroTEM detected the Deposit on all three flight lines. The fixed-wing system detected the Deposit only on two flight lines. In exploration programs that seek to expand the flight line spacing in an effort to reduce the cost of the airborne survey, discrete conductors such as the Mesamax Deposit can go undetected. The argument often put forward in favour of using fixed-wing systems is that because of their larger footprint, the flight line spacing can indeed be widened. Many fixed-wing surveys are flown at 200 m or 400 m. Much of the survey work performed by Aeroquest has been to survey in areas that were previously flown at these wider line spacings. One of the reasons for AeroTEM's impressive discovery record has been the strategy of flying closely spaced lines and finding all the discrete near-surface conductors. These higher resolution surveys are being flown within existing mining camps, areas that improve the chances of discovery.

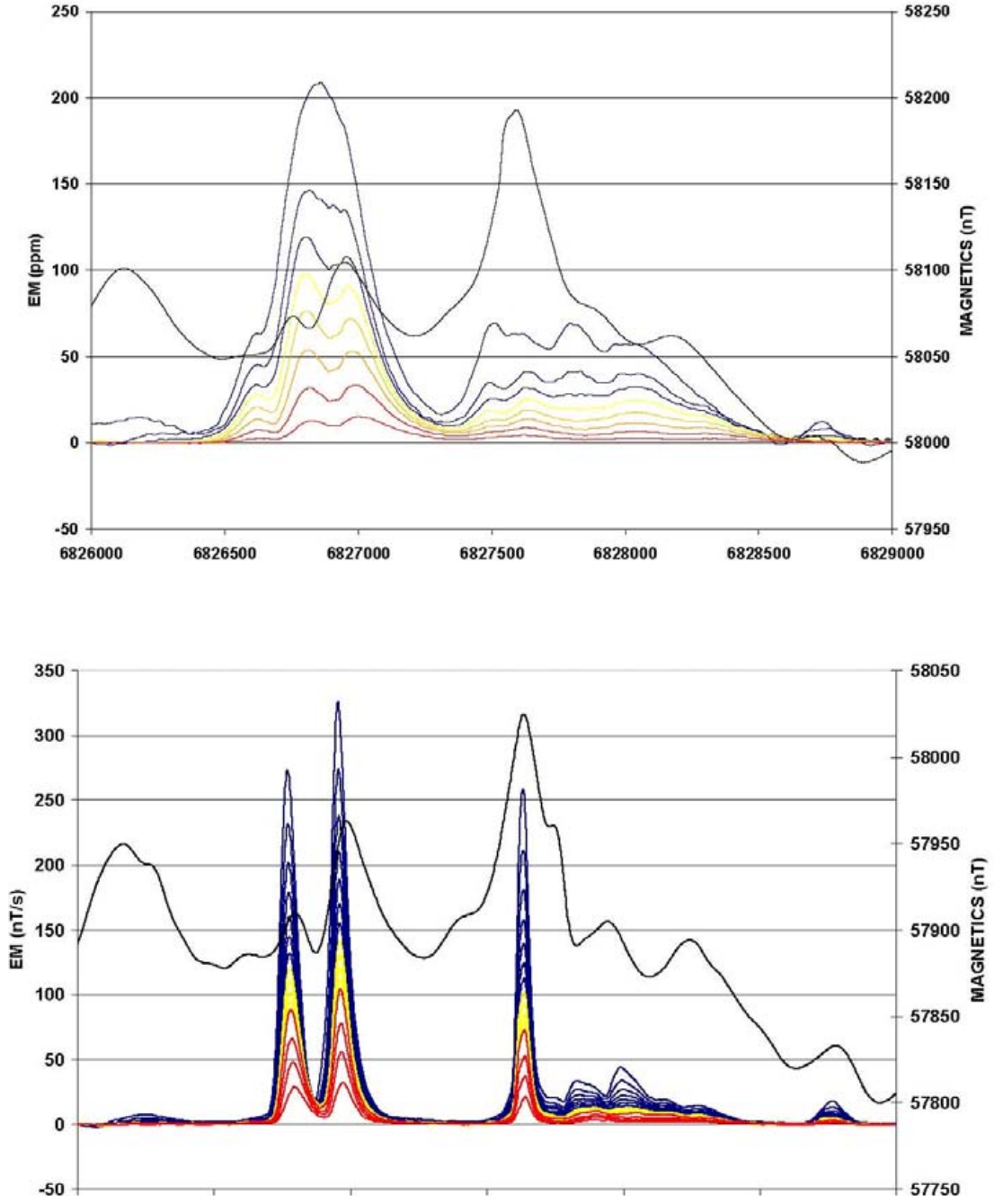

Figure 2. Fixed-wing (upper) and AeroTEM (lower) comparison over the eastern limit of the Mesamax Deposit, a Ni-Cu-PGE zone located in the Raglan nickel belt and owned by Canadian Royalties. Both systems detected the Deposit further to the west where it is closer to surface.

The small footprint of AeroTEM combined with the high signal to noise ratio (S/N) makes the system more

suitable to surveying in areas where local infrastructure produces electromagnetic noise, such as power lines and railways. In 2002 Aeroquest flew four exploration properties in the Sudbury Basin that were under option by FNX Mining Company Inc. from Inco Limited. One such property, the Victoria Property, contained three major power line corridors.

The resulting AeroTEM survey identified all the known zones of Ni-Cu-PGE mineralization, and detected a response between two of the major power line corridors but in an area of favourable geology. Three boreholes were drilled to test the anomaly, and all three intersected sulphide. The third borehole encountered 1.3% Ni, 6.7% Cu, and 13.3 g/t TPMs over 42.3 ft. The mineralization was subsequently named the Powerline Deposit.

The success of AeroTEM in Sudbury highlights the advantage of having a system with a small footprint, but also one with a high S/N. This latter advantage is achieved through a combination of a high-moment (high signal) transmitter and a rigid geometry (low noise). Figure 3 shows the Powerline Deposit response and the response from the power line corridor at full scale. The width of power line response is less than 75 m.

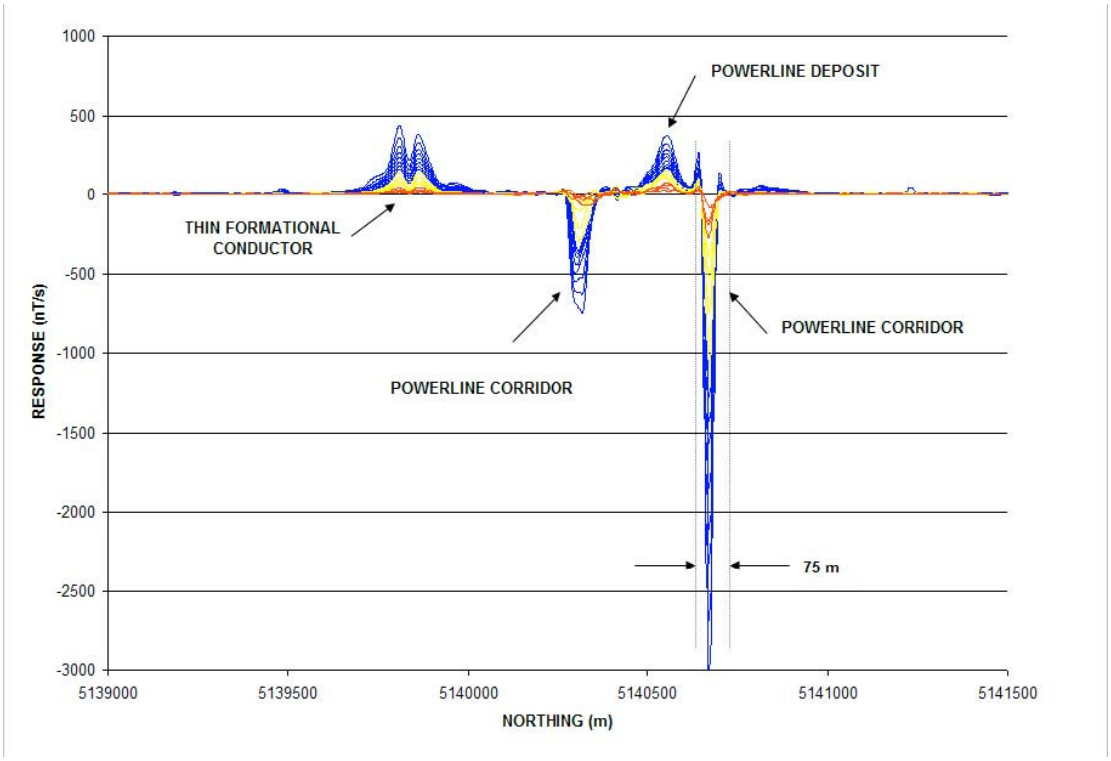

Figure 3. The Powerline Deposit is located between two major power line corridors, which make EM surveying problematic. Despite the strong response from the power line, the anomaly from the Deposit is clearly detected. Note the thin formational conductor located to the south. The only way to distinguish this response from that of two closely spaced conductors is by interpreting the X-axis coil response.

Advantage 2 – Conductance Discrimination

The AeroTEM system features full waveform recording and as such is able to measure the on-time response due to high conductance targets. Due to the processing method (primary field removal), there is attenuation of the response with increasing conductance, but the AeroTEM on-time measurement is still superior to systems that rely on lower base frequencies to detect high conductance targets, but do not measure in the on-time.

The peak response of a conductive target to an EM system is a function of the target conductance and the EM system base frequency. For time domain EM systems that measure only in the off-time, there is a drop in the peak response of a target as the base frequency is lowered for all conductance values below the peak system response. For example, the AeroTEM peak response occurs for a 10 S conductor in the early off-time and 100 S

in the late off-time for a 150 Hz base frequency. Because base frequency and conductance form a linear relationship when considering the peak response of any EM system, a drop in base frequency of 50% will double the conductance at which an EM system shows its peak response. If the base frequency were lowered from 150 Hz to 30 Hz there would be a fivefold increase in conductance at which the peak response of an EM occurred.

However, in the search for highly conductive targets, such as pyrrhotite-related Ni-Cu-PGM deposits, a fivefold increase in conductance range is a high price to pay because the signal level to lower conductance targets is reduced by the same factor of five. For this reason, EM systems that operate with low base frequencies are not suitable for general exploration unless the target conductance is more than 100 S, or the target is covered by conductive overburden.

Despite the excellent progress that has been made in modeling software over the past two decades, there has been little work done on determining the optimum form of an EM system for mineral exploration. For example, the optimum configuration in terms of geometry, base frequency and so remain unknown. Many geophysicists would argue that there is no single ideal configuration, and that each system has its advantages and disadvantages. We disagree.

When it comes to detecting and discriminating high-conductance targets, it is necessary to measure the pure in phase response of the target conductor. This measurement requires that the measured primary field from the transmitter be subtracted from the total measured response such that the secondary field from the target conductor can be determined. Because this secondary field is in-phase with the transmitter primary field, it must be made while the transmitter is turned on and the transmitter current is changing. The transmitted primary field is several orders of magnitude larger than the secondary field. AeroTEM uses a bucking coil to reduce the primary field at the receiver coils. The only practical way of removing the primary field is to maintain a rigid geometry between the transmitter, bucking and receiver coils. This is the main design consideration of the AeroTEM airframe and it is the only time domain airborne system to have this configuration.

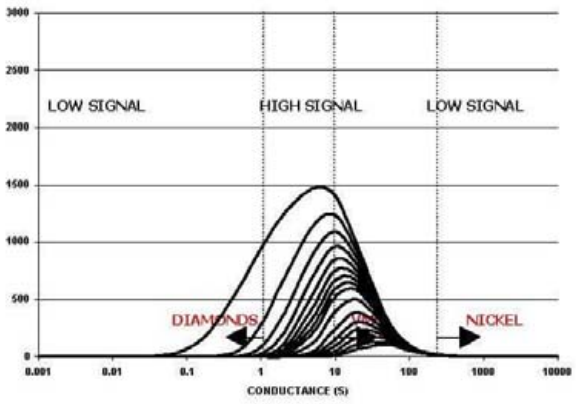

The off-time AeroTEM response for the 16 channel configuration.

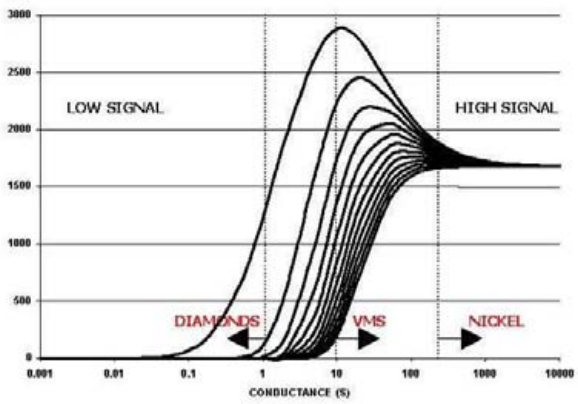

The on-time response assuming 100% removal of the measured primary field.

Figure 4. The off-time and on-time response nomogram of AeroTEM for a base frequency of 150 Hz. The on-time response is much stronger for higher conductance targets and this is why on-time measurements are more important than lower frequencies when considering high conductance targets in a resistive environment.

Advantage 3 – Multiple Receiver Coils

AeroTEM employs two receiver coil orientations. The Z-axis coil is oriented parallel to the transmitter coil and both are horizontal to the ground. This is known as a maximum coupled configuration and is optimal for detection. The X-axis coil is oriented at right angles to the transmitter coil and is oriented along the line-of-flight. This is known as a minimum coupled configuration, and provides information on conductor orientation and

thickness. These two coil configurations combined provide important information on the position, orientation, depth, and thickness of a conductor that cannot be matched by the traditional geometries of the HEM or fixed-wing systems. The responses are free from a system geometric effect and can be easily compared to model type curves in most cases. In other words, AeroTEM data is very easy to interpret. Consider, for example, the following modeled profile:

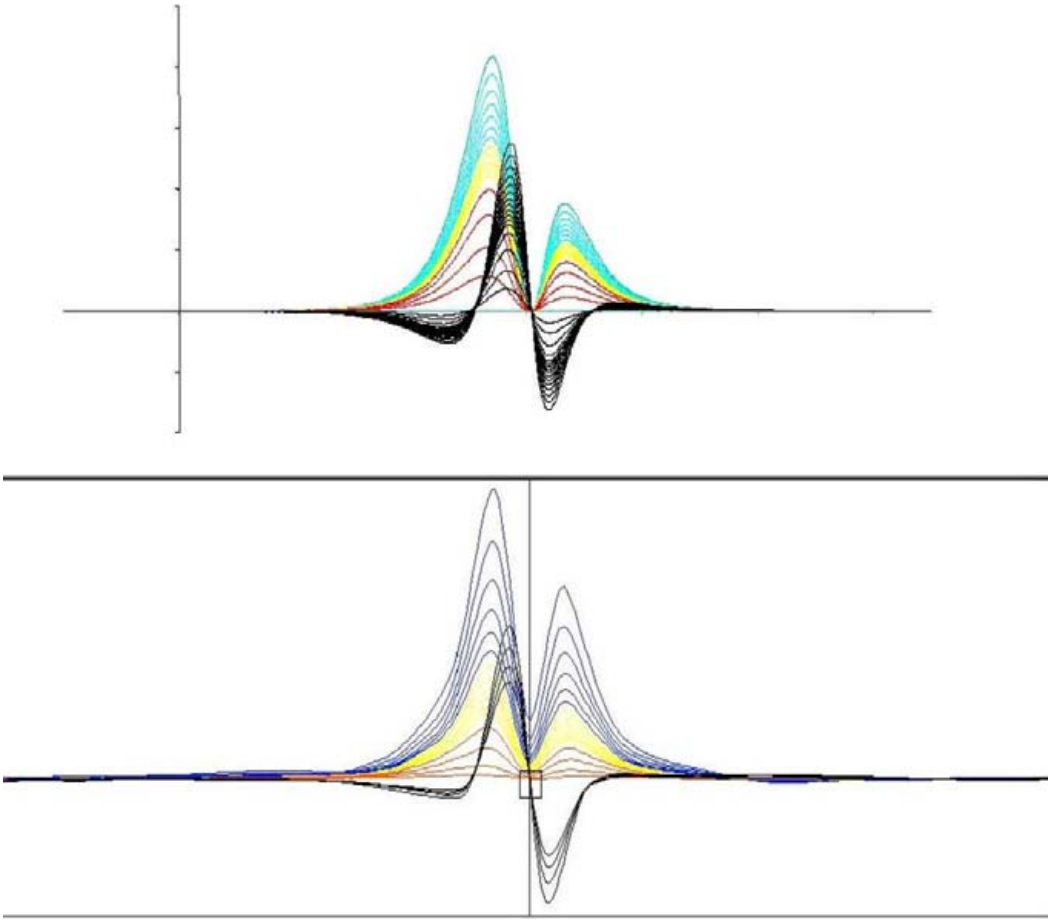

Figure 5. Measured (lower) and modeled (upper) AeroTEM responses are compared for a thin steeply dipping conductor. The response is characterized by two peaks in the Z-axis coil, and a cross-over in the X-axis coil that is centered between the two Z-axis peaks. The conductor dips toward the higher amplitude Z-axis peak. Using the X-axis cross-over is the only way of differentiating the Z-axis response from being two closely spaced conductors.

HEM versus AeroTEM

Traditional helicopter EM systems operate in the frequency domain and benefit from the fact that they use narrowband as opposed to wide-band transmitters. Thus all of the energy from the transmitter is concentrated in a few discrete frequencies. This allows the systems to achieve excellent depth penetration (up to 100 m) from a

transmitter of modest power. The Aeroquest Impulse system is one implementation of this technology.

The AeroTEM system uses a wide-band transmitter and delivers more power over a wide frequency range. This frequency range is then captured into 16 time channels, the early channels containing the high frequency information and the late time channels containing the low frequency information down to the system base frequency. Because frequency domain HEM systems employ two coil configurations (coplanar and coaxial) there are only a maximum of three comparable frequencies per configuration, compared to 16 AeroTEM off-time and 12 AeroTEM on-time channels.

Figure 6 shows a comparison between the Dighem HEM system (900 Hz and 7200 Hz coplanar) and AeroTEM (Z-axis) from surveys flown in Raglan, in search of highly conductive Ni-Cu-PGM sulphide. In general, the AeroTEM peaks are sharper and better defined, in part due to the greater S/N ratio of the AeroTEM system over HEM, and also due to the modestly filtered AeroTEM data compared to HEM. The base levels are also better defined in the AeroTEM data. AeroTEM filtering is limited to spike removal and a 5-point smoothing filter. Clients are also given copies of the raw, unfiltered data.

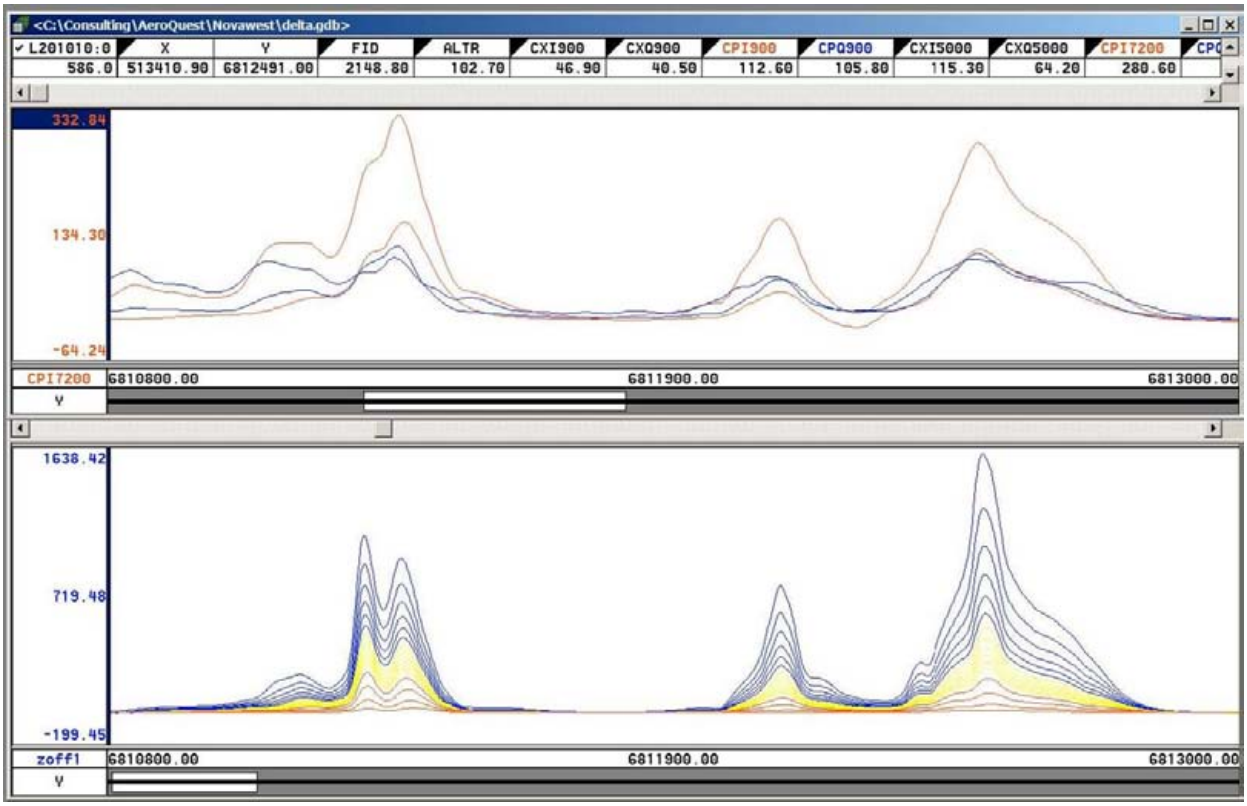

Figure 6. Comparison between Dighem HEM (upper) and AeroTEM (lower) surveys flown in the Raglan area. The AeroTEM responses appear to be more discrete, suggesting that the data is not as heavily filtered as the HEM data. The S/N advantage of AeroTEM over HEM is about 5:1.

Aeroquest Limited is grateful to the following companies for permission to publish some of the data from their respective surveys: Wolfden Resources, FNX Mining Company Inc, Canadian Royalties, Nova West Resources, Aurogin Resources, Spectrem Air. Permission does not imply an endorsement of the AeroTEM system by these companies.

APPENDIX 5: AEROTEM INSTRUMENTATION SPECIFICATION SHEET

AEROTEM Helicopter Electromagnetic System

System Characteristics

- Transmitter: Triangular Pulse Shape Base Frequency 90 Hz
- Tx On Time – 1,833 (90 Hz) µs
- Tx Off Time – 3,667 (90 Hz) µs
- Loop Diameter - 10 m
- Peak Current - 455 A
- Peak Moment – 183,131 NIA
- Typical Z Axis Noise at Survey Speed = 5 nT/s peak to peak
- Sling Weight: 1000 lb
- Length of Tow Cable: 56.1 m
- Bird Survey Height: 30 m nominal

Receiver

- Two Axis Receiver Coils (x, z) positioned at centre of transmitter loop
- Selectable Time Delay to start of first channel 21.3 , 42.7, or 64.0 ms

Display & Acquisition

- AERODAS Digital recording at 120 samples per decay curve at a maximum of 300 curves per second (27.778 µs channel width)
- RMS Channel Widths: 52.9,132.3, 158.7, 158.7, 317.5, 634.9 µs
- Recording & Display Rate = 10 readings per second.
- On-board display - six channels Z-component and 1 X-component

System Considerations

Comparing a fixed-wing time domain transmitter with a typical moment of 500,000 NIA flying at an altitude of 120 m with a Helicopter TDEM at 30 m, notwithstanding the substantial moment loss in the airframe of the fixed wing, the same penetration by the lower flying helicopter system would only require a sixty-fourth of the moment. Clearly the AeroTEM system with nearly 183.131 NIA has more than sufficient moment. The airframe of the fixed wing presents a response to the towed bird, which requires dynamic compensation. This problem is non-existent for AeroTEM since transmitter and receiver positions are fixed. The AeroTEM system is completely portable, and can be assembled at the survey site within half a day.

APPENDIX 2

MAPS

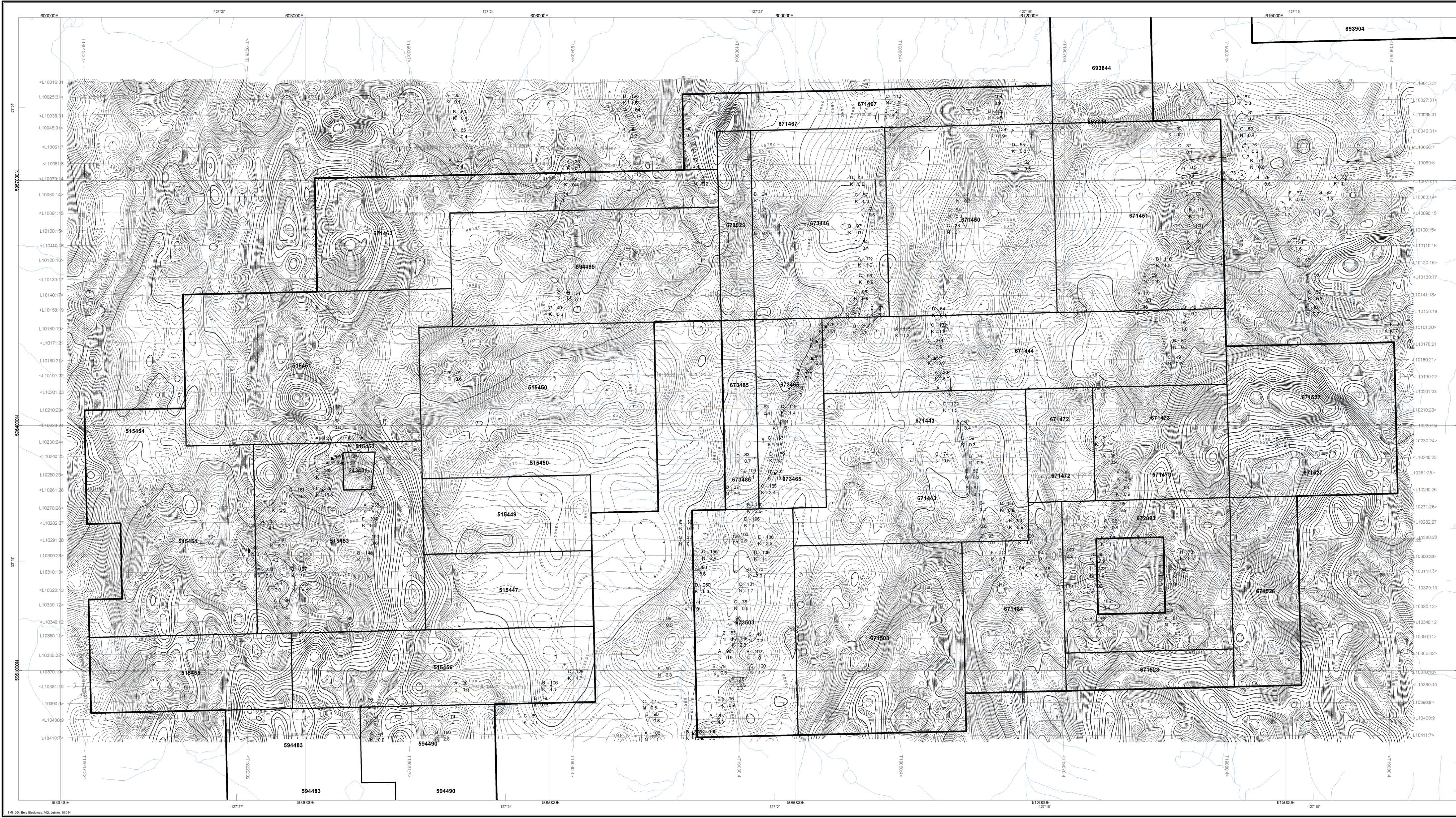

Grid North
NAD83 - Zone09N

The topographic data base was sourced from client 1:20,000 scale

Background shading derived from NASA SRTM data
Inset data derived from Natural Resources Canada 'Atlas of Canada Base Maps'

This map accompanies the technical report entitled 'Report on a Helicopter-Borne Magnetic and Electromagnetic Survey, Smithers, British Columbia', by Aeroquest Limited, November 2010

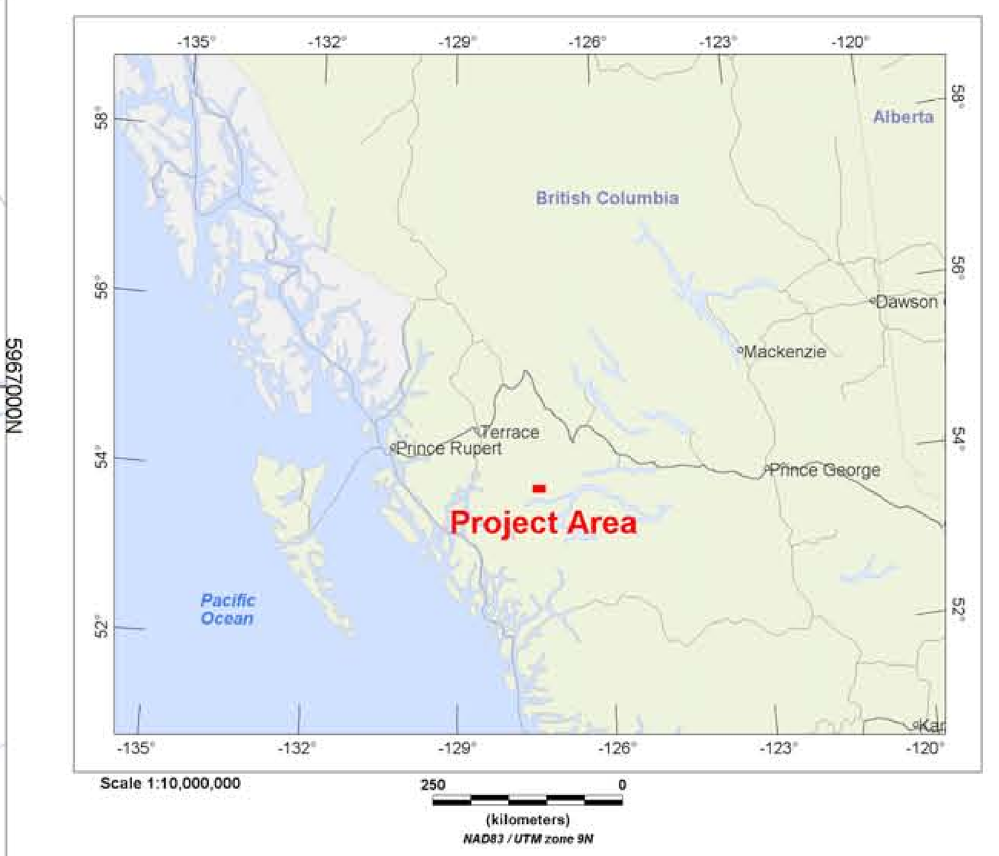

Scale 1:10,000,000
250 0
(kilometers)
NAD83 / UTM zone 9N

Off-Time Anomaly Symbols

- >50S
- 35-50S
- 20-35S
- 10-20S
- 5-10S
- 1-5S
- <1S

anomaly label A, 125 decay constant (µs)
thicK/thiN source K, 36 off-time conductance (S)

Contour Interval

- 10 nT
- 20 nT
- 100 nT
- 500 nT

- Topographic Contour
- Road
- River
- Lake

SURVEY SPECIFICATIONS:
Survey flown: August 8 - 14, 2010
Traverse/Tie line spacing: 200/2000 metres
Traverse/Tie line direction: 90°/0°
Nominal EM bird height: 30 metres
Aircraft: Aerospatiale SA 315B (C-GLOV)
INSTRUMENTATION:
Data acquisition: ADAS
Magnetometer: Geometrics G-823A caesium vapour
Installation: Towed bird 38 m above EM bird
Sensitivity: .001 nanoTesla
Electromagnetics: AeroTEM III System (November)
Configuration: Towed bird
NAVIGATION:
Navigation: Differential Global Positioning System (DGPS)
Navigation equipment: AGNAV with MID-TECH RX400p receiver
Radar Altimeter: Terra TRA3000/TRI-30
POSITIONING
Datum: NAD83
Major Axis: 6378137.000
Eccentricity: 0.081819191
MAP PROJECTION
Projection: Universal Transverse Mercator
Central Meridian: 129°W (Zone 09)
Central Scale Factor: 0.9996
False Easting/Northing: 500,000m/0m

scale 1:20,000
250 0 250 500 750 1000 1250 1500
(meters)
NAD83 / UTM zone 9N

Terrane Metals Corp.
Smithers, British Columbia

TOTAL MAGNETIC INTENSITY

Berg Block

NTS 093E14

AEROQUEST
7687 Bath Road, Mississauga, ON, Canada, L4T 3T1
Tel: (905) 672-9129 Fax: (905) 672-7083
www.aeroquest.ca

November 2010

TMI

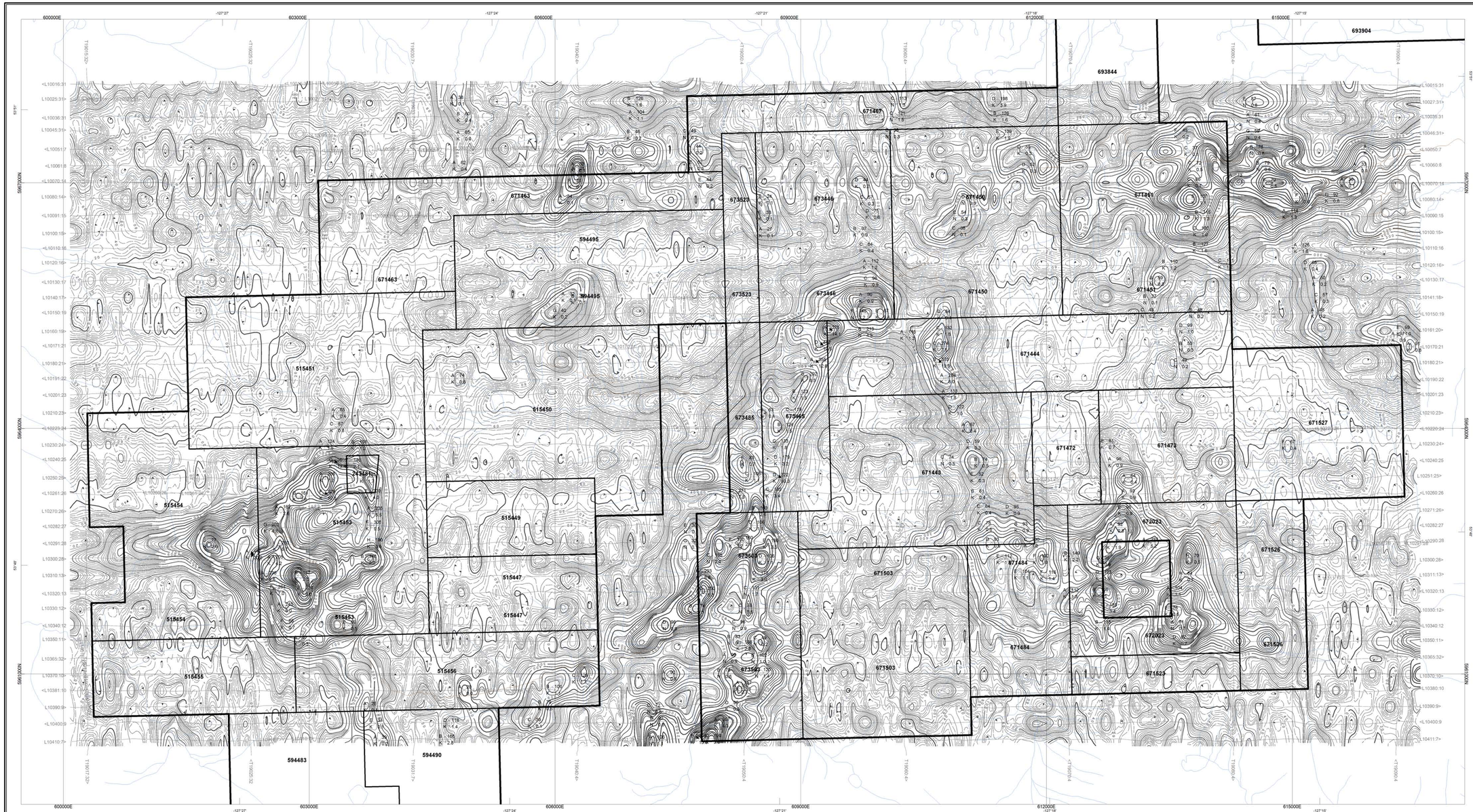

The topographic data base was sourced from client 1:20,000 scale

Background shading derived from NASA SRTM data
Inset data derived from Natural Resources Canada 'Atlas of Canada Base Maps'

This map accompanies the technical report entitled 'Report on a Helicopter-Borne Magnetic and Electromagnetic Survey, Smithers, British Columbia', by Aeroquest Limited, November 2010

Grid North
NAD83 - Zone09N

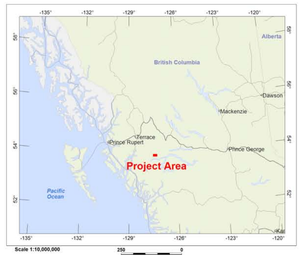

Off-Time Anomaly Symbols

- >50S
- 35-50S
- 20-35S
- 10-20S
- 5-10S
- 1-5S
- <1S

anomaly label — decay constant (µs) — thickn'ONN source — off-time conductance (S)

Contour Interval

- 10 nT/s
- 20 nT/s
- 100 nT/s
- 500 nT/s

Topographic Contour
Road
River
Lake

SURVEY SPECIFICATIONS:
Survey flown: August 8 - 14, 2010
Traverse/Tie line spacing: 200/2000 metres
Traverse/Tie line direction: 90°/0°
Nominal EM bird height: 30 metres
Aircraft: Aerospatiale SA 315B (C-GLOV)
INSTRUMENTATION:
Data acquisition: ADAS
Magnetometer: Geometrics G-823A caesium vapour
Installation: Towed bird 38 m above EM bird
Sensitivity: .001 nanoTesla
Electromagnetics: AeroTEM III System (November)
Configuration: Towed bird
NAVIGATION:
Navigation: Differential Global Positioning System (DGPS)
Navigation equipment: ACNAV with MID-TECH RX400p receiver
Radar Altimeter: Terra TRA3000/TRI-30
POSITIONING
Datum: NAD83
Major Axis: 6378137.000
Eccentricity: 0.081819191
MAP PROJECTION
Projection: Universal Transverse Mercator
Central Meridian: 129°W (Zone 09)
Central Scale Factor: 0.9996
False Easting/Northing: 500,000m/0m

scale 1:20,000

(metres)
NAD83 / UTM zone 9N

Terrane Metals Corp.
Smithers, British Columbia

AEROTEM Z1-OFF TIME
Time after Tx Off 65 µs
Berg Block

NTS 093E14

AEROQUEST
7687 Bath Road, Mississauga, ON, Canada, L4T 3T1
Tel: (905) 672-9129 Fax: (905) 672-7083
www.aeroquest.ca

November 2010

ZOFF1

ZOFF1_20k_Berg Block.map, AQL Job no. 10-044

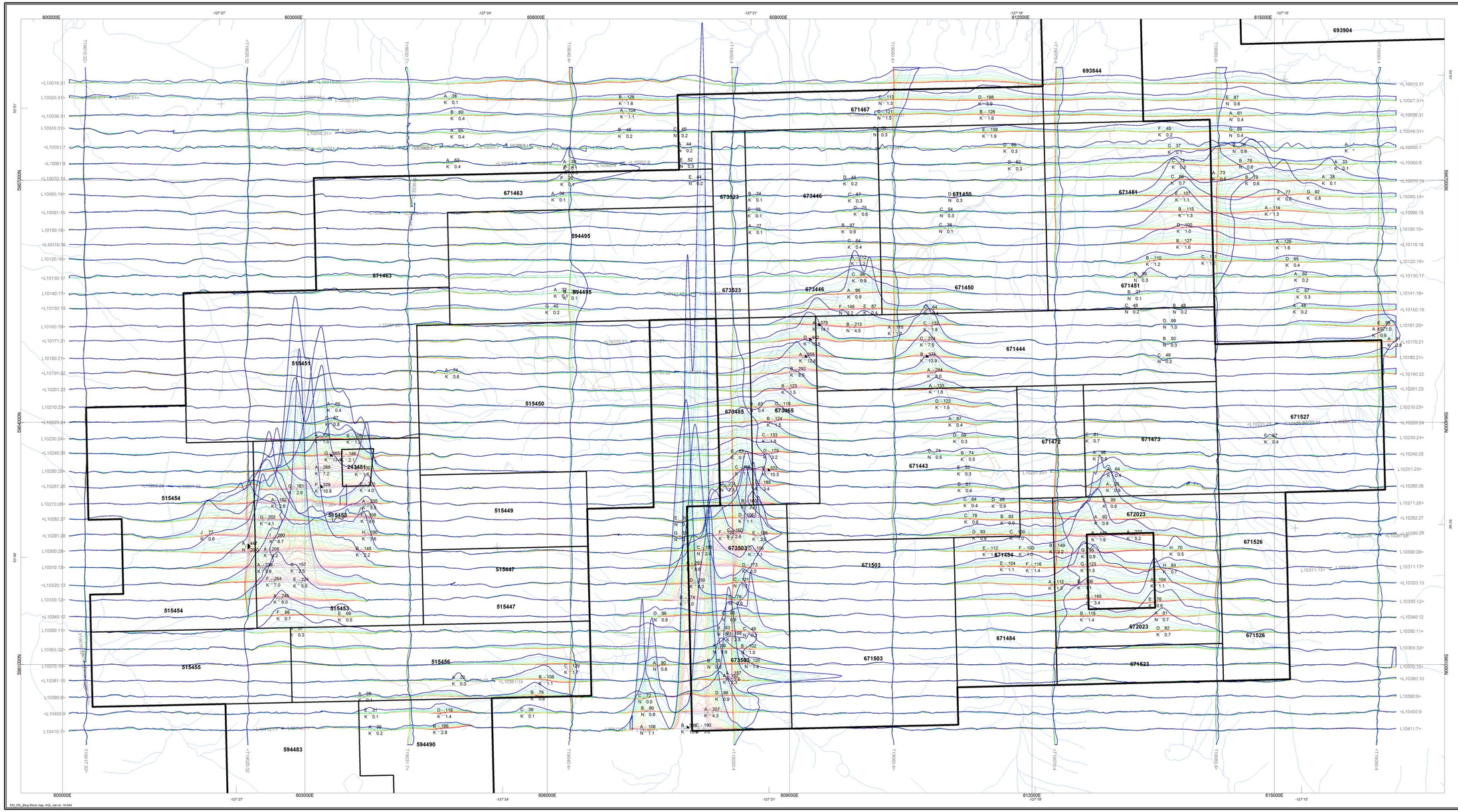

The topographic data base was sourced from client 1:20,000 scale

Background shading derived from NASA SRTM data
Inset data derived from Natural Resources Canada 'Atlas of Canada Base Maps'

This map accompanies the technical report entitled 'Report on a Helicopter-Borne Magnetic and Electromagnetic Survey, Smithers, British Columbia', by Aeroquest Limited, November 2010

Grid North
NAD83 - Zone09N

Scale 1:10,000,000
200 0 (kilometers)
NAD83 / UTM zone 9N

AeroTEM Z Off-Time Profiles
positive excursion to top and right, 1mm=30nT/s

- Z3 Off-Time Channel 120.5 µs
- Z4 Off-Time Channel 148.3 µs
- Z5 Off-Time Channel 176.1 µs
- Z6 Off-Time Channel 231.7 µs
- Z7 Off-Time Channel 315.0 µs
- Z8 Off-Time Channel 398.3 µs
- Z9 Off-Time Channel 481.7 µs
- Z10 Off-Time Channel 592.8 µs
- Z11 Off-Time Channel 731.7 µs
- Z12 Off-Time Channel 898.3 µs
- Z13 Off-Time Channel 1134.4 µs

Off-Time Anomaly Symbols

- >50S
- 35-50S
- 20-35S
- 10-20S
- 5-10S
- 1-5S
- <1S

anomaly label: thickness source, decay constant (µs), off-time conductance (S)

- Topographic Contour
- Road
- River
- Lake

SURVEY SPECIFICATIONS:
Survey flown: August 8 - 14, 2010
Traverse/Tie line spacing: 200/2000 metres
Traverse/Tie line direction: 90°/0°
Nominal EM bird height: 30 metres
Aircraft: Aerospatiale SA 315B (C-GLOV)
INSTRUMENTATION:
Data acquisition: ADAS
Magnetometer: Geometrics G-823A caesium vapour
Installation: Towed bird 38 m above EM bird
Sensitivity: .001 nanoTesla
Electromagnetics: AeroTEM III System (November)
Configuration: Towed bird
NAVIGATION:
Navigation: Differential Global Positioning System (DGPS)
Navigation equipment: AGNAV with MID-TECH RX400p receiver
Radar Altimeter: Terra TRA3000/TRI-30
POSITIONING
Datum: NAD83
Major Axis: 6378137.000
Eccentricity: 0.081819191
MAP PROJECTION
Projection: Universal Transverse Mercator
Central Meridian: 129°W (Zone 09)
Central Scale Factor: 0.9996
False Easting/Northing: 500,000m/0m

scale 1:20,000
250 0 250 500 750 1000 1250 1500 (meters)
NAD83 / UTM zone 9N

Terrane Metals Corp.
Smithers, British Columbia

AEROTEM
OFF TIME PROFILES
Berg Block

NTS 093E14

AEROQUEST
7687 Bath Road, Mississauga, ON, Canada, L4T 3T1
Tel: (905) 672-9129 Fax: (905) 672-7083
www.aeroquest.ca

November 2010

EM

APPENDIX 3

STATEMENT OF EXPENDITURES

Exploration Work type	Comment	Days			Totals
Office Studies	**List Personnel (note - Office only, do not include field days**				
Literature search			$0.00	$0.00	
Database compilation			$0.00	$0.00	
Planning / Supervision	Sergio Espinosa	6.7	$650.00	$4,350.00	
Reprocessing of data	Darren O'Brien	5.0	$650.00	$3,250.00	
General research			$0.00	$0.00	
Report preparation	Darin Labrenz	6.0	$650.00	$3,900.00	
Other (specify)				$0.00	
				$11,500.00	**$11,500.00**
Airborne Exploration Surveys					
Aeromagnetics			$0.00	$0.00	
Radiometrics			$0.00	$0.00	
Electromagnetics	754.35 line km		$0.00	$88,394.00	
Gravity			$0.00	$0.00	
Digital terrain modelling			$0.00	$0.00	
Other (specify)			$0.00	$0.00	
				$88,394.00	**$88,394.00**
TOTAL Expenditures					**$99,894.00**